EFFECTIVENESS OF ENERGY DISSIPATION DEVICES FOR SEISMIC RESPONSE OF BUILDING

BY

Nelson N. Macwan

10MCLC021

DEPARTMENT OF CIVIL ENGINEERING

AHMEDABAD-382481

May 2012

EFFECTIVENESS OF ENERGY DISSIPATION DEVICES
FOR SEISMIC RESPONSE OF BUILDING

Major Project

Submitted in partial fulfillment of the requirements

For the degree of

Master of Technology in Civil Engineering

(Computer Aided Structural Analysis & Design)

By

NELSON N. MACWAN

10MCLC021

DEPARTMENT OF CIVIL ENGINEERING

AHMEDABAD-382481

May 2012

Declaration

This is to certify that

a. The thesis comprises my original work towards the Degree of Master of Technology in Civil Engineering (Computer Aided Structural Analysis and Design) at Nirma University and has not been submitted elsewhere for a degree.

b. Due acknowledgement has been made in the text to all other material used.

Nelson N. Macwan

Certificate

This is to certify that the Major Project entitled "EFFECTIVENESS OF ENERGY DISSIPATION DEVICES FOR SEISMIC RESPONSE OF BUILDING" submitted by Nelson N. Macwan (10MCLC021), towards the partial fulfillment of the requirements for the degree of Master of Technology in Civil Engineering (Computer Aided Structural Analysis and Design) of Nirma University, Ahmedabad is the record of work carried out by him under my supervision and guidance. In my opinion, the submitted work has reached a level required for being accepted for examination. The results embodied in this major project, to the best of my knowledge, haven't been submitted to any other university or institution for award of any degree or diploma.

Dr. S.P. Purohit
Guide and Associate Professor,
Department of Civil Engineering,
Institute of Technology,
Nirma University, Ahmedabad

Dr. P. H. Shah
Professor and Head,
Department of Civil Engineering,
Institute of Technology,
Nirma University, Ahmedabad

Dr K Kotecha
Director,
Institute of Technology,
Nirma University,
Ahmedabad

____
Examiner

____
Date of Examintion

Abstract

In order to control the vibration response of buildings during earthquakes, passive energy dissipation devices are most commonly used.These devices provide an additional damping to building, which helps in reducing seismic response of it. There are a number of types of dampers available, which use a variety of materials to obtain different levels of damping. These include dampers like viscous, viscoelastic(VE), Metallic, friction and magneto-rheological(MR) damper. These dampers are usually placed between framing elements at various storey.

Present study considers seismic response reduction of three storey shear building using passive energy dissipation devices i.e. friction damper and semi-active device, magneto-rheological(MR) damper used passively placed at ground floor only. Behaviour of friction and MR damper was studied by characterizing these devices under sinusoidal and random elicitation, analytically.

A three storey shear building has been considered. A lump mass model approach is used to obtain mass and stiffness matrices. Damping is assumed to be Rayleigh's type and damping matrix is determined considering 5 % critical damping co-efficient for all modes. Equation of motion for three storey building with damper attached at G.F. The equation of motion derived, are solved using Newmark-Beta and Runge-Kutta method respectively for building with friction and MR dampers through MATLAB. Four different type of earthquakes namely, El centro(1940), Kobe(1995), Loma Prieta(1989) and Northridge(1994) are used to determine uncontrolled(building without damper) response for the building. Response quantities like displacement, velocity, acceleration, inter storey drift were extracted for uncontrolled and controlled(with dampers) building. The response quantities of uncontrolled building have been compared with the controlled building in order to establish efficiency of friction and MR damper.

It has been found that all response quantities shows reduction for controlled building as compared to uncontrolled building. It was found that friction damper is most effective under Northridge type of excitation. It is also noted that MR damper considered in present study reduces response quantities of controlled building marginally when used in "Passive Off" condition, i.e. like viscous damping. However, MR damper keeps in reducing response quantities of controlled building substantially when used as "Passive On" condition, i.e voltage of 2.5 V applied continuously.

Acknowledgements

I would first of all like to thanks **Dr. S. P. Purohit**, Guide M.Tech. Department of Civil Engineering (CASAD), Institute of Technology, Nirma University, Ahmedabad whose keen interest and excellent knowledge base helped me to carry out the dissertation work. His constant support and interest in the subject equipped me with a great understanding of different aspects of the required architecture for the project work. He has shown keen interest in this dissertation work right from beginning and has been a great motivating factor in outlining the flow of my work.

My sincere thanks and gratitude to **Dr. P. V. Patel**, Professor, Department of Civil Engineering, and **Prof. N. C. Vyas**, Professor, Civil Engineering Department, Institute of Technology, Nirma University, Ahmedabad for his continual kind words of encouragement and motivation throughout the Dissertation work.

I further extend my thanks to **Dr. P. H. Shah**, Head, Department of Civil Engineering, Institute of Technology, Nirma University, Ahmedabad and **Dr K Kotecha**, Director, Institute of Technology, Nirma University, Ahmedabad for providing all kind of required resources during my study.

I would like to thank The Almighty, my family and all my friends, for supporting and encouraging me in all possible ways throughout the dissertation work.

- Nelson N. Macwan

10MCLC021

Abbreviation Notation and Nomenclature

ADAS .... Added Damping and Stiffness
DVA .... Dynamic Vibration Absorber
EQ .... Earthquake
FEMA .... Federal Emergency Management Egency
HMD .... Hybrid Mass Damper
TMD .... Tuned Mass Damper
PGA .... Peak Ground Acceleration
PGV .... Peak Ground Velocity
PGD .... Peak Ground Displacement
sgm .... Signum Function
RCC .... Reinforced Cement Concrete
SDOF .... Single Degree of Freedom
VE .... Viscoelastic
a .... Amplitude of Motion
m .... Mass Matrix of Building
k .... Stiffness Matrix of Building
c .... Damping Matrix of Building
f_{ck} .... Characteristic Strength of Concrete
f_y .... Characteristic Strength of Steel
E_d .... Energy Dissipation per Cycle
γ_0 .... Shear Strain Amplitude
V .... Volume of the Viscoelastic Material
P(t) .... Force in an Energy Dissipation Damper as a Function of Time
C_d .... Co-efficient of Damper
α .... Evolutionary coefficient
γ,β and A .... Hysteresis parameters
u .... Output of First Order Filter
v .... Command Voltage

c_0 and c_1 .... Coefficient of Damping for Proposed Bouc-Wen Model

k_1 .... Accumulator Stiffness

f .... Circular Frequency(Radians per Seconds)

G' .... Storage Modulus of Viscoelastic Material

G'' .... Loss Modulus of Viscoelastic Material

K_d .... Damper Stiffness of VE Damper

$F(t)$ .... Force in Damper

Contents

List of Tables

List of Figures

Chapter 1

Introduction

1.1 General

In recent years, due to development in design methodology and newer material with high performance qualities, structures become lighter, taller and slender. These structures are dynamically response when subjected to dynamic loads such as Earthquake, wind etc. Dynamic response of such structures needs to be controlled to resist excessive stress and loads. This is addressed by an advance technology in civil engineering called "Structural Vibration Control", which modifies dynamic properties of structure and safeguard to it. Structural Control is a diverse field of study which involves various ways to modify to properties of structural vibration control that found promising is to install mechanical system, i.e damper in the structure.

This helps in modifying stiffness and/or damping properties of structure which is responsible for dynamic response to external excitations. Note that, every structure do posses inherent damping known as structural damping, which helps it to resist vibration to some extent which are caused to excitation. However under strong excitation, this damping is not sufficient to mitigate structural response. Most civil structures have damping coefficient ranges between 2 % to 20 % of critical damping coefficient. This is damping level may not be good enough when they are subjected to strong excitation and needs additional damping to reduce structural response. Various structural control approach are recently desired. They are broadly classified as base isolation system, passive control system, active control system and hybrid control system.

However inherent or natural damping in structure helps to a some extent vibrations caused due to earthquake etc. But, for structures subjected to strong motions, the inherent damping in the structure is not sufficient to mitigate the structural response. All vibrating structures dissipate energy due to internal stressing, rubbing, cracking, plastic deformations, and so on; the larger the energy dissipation capacity the smaller the amplitudes of vibration. Some structures have very low damping on the order of 1% of critical damping and consequently experience large amplitudes of vibration even for moderately strong earthquakes. In this regard, many researchers have studied, developed and tested different supplemental damping techniques.

The control of structural vibrations produced by earthquake or wind can be done by various means such as modifying rigidities, masses, damping, or shape, and by providing passive or active counter forces. Structural control methods that can be used include:

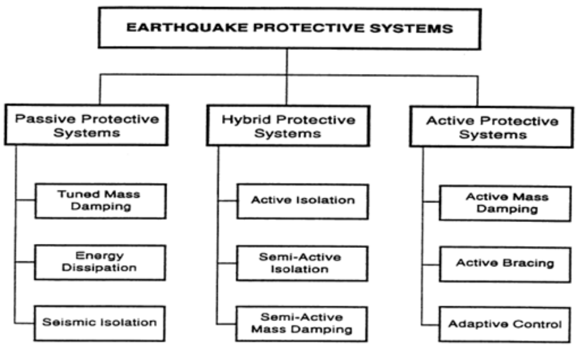

Figure 1.1: Earthquake Protective Systems

The concept behind base isolation is to detach (isolate) the building from the ground in such a way that earthquake motions are not transmitted up through the building or at least greatly reduced.
A passive control system does not require an external power source.Passive control devices impart forces that are developed in response to the motion of the structure as shown. The passive control devices cannot increase the energy in a passively controlled structural system, including the passive devices. Passive energy dissipation devices can be effective against wind and earthquake induced motion, and generally operates on principles such as, yielding of metals, frictional sliding and deformation of viscoelastic (VE) solids or fluids.
An active control system is one in which an external source powers control actuator that apply forces to the structure in a prescribed manner. These forces can be used to both add stiffness, damping and dissipate energy in the structure.

Semi-active control have been studied by many researchers. It combines active and passive control systems and attempts to utilize the advantages of both methods to achieve better effects. Semi-active control systems combine the features of active and passive control to reduce the response of structures to various dynamic loadings. Semi-active control systems are a class of active control systems for which the external energy requirements are orders of magnitude smaller than typical active control systems.

Typically, semi-active control devices do not add mechanical energy to the structural system (including the structure and the control actuators), therefore bounded-input bounded-output is guaranteed. Semi-active control devices are often viewed as controllable passive devices.

Active/hybrid control systems are force delivery devices integrated with real-time processing evaluators/controllers and sensors within the structure. They act simultaneously with the hazardous excitation to provide enhanced structural behavior for improved service and safety.

In order to control the vibration response of buildings during earthquakes, energy absorbing passive damping devices are most commonly used for dissipating energy. Nowadays there are number of manufacturing companies which are making dampers available in the market. Some of these include Friction, Metallic, Viscoelastic and Viscous Dampers. An effective damping system can result in higher levels of safety and comfort; and can also lead to considerable savings in total cost of a building.

1.2 Background

Recently, concept of structural control has employed for a safer and economical design of the structural system using active control, passive control, and hybrid control devices, These devices yields reduction in response of buildings subjected to earthquake ground motions. Passive control devices were developed the earliest and have been used more commonly in practice for seismic design because they require minimum maintenance and need no external power supply to operate.

The concept of structural control as currently defined can trace its roots back more than 100 years to John Milne, a professor of engineering in Japan, who built a small house of wood and placed it on ball bearings to demonstrate that a structure could be isolated from earthquake shaking. The development of linear system theory and its application to the field of vibration, and in particular structural dynamics, required much of the first half of the twentieth century. The driving force for much of this development was the internal combustion engine, used in both automobiles and airplanes, which inherently produced significant dynamic force levels at connection points. It was during the 2nd world war that concepts such as vibration isolation, vibration absorption, and vibration damping were developed and effectively applied to aircraft structures.

1.3 Objective of Study

The main objective of present study is how to reduce response of building subjected to various earthquake excitations using passive energy dissipation devices like friction damper and MR damper. Also, compare the performances of controlled building with respect to uncontrolled structure. The specific objectives stated as follows:

- To study passive energy dissipation devices and their principle. Study in detail mathematical modeling of these devices, and understand the influence of various model parameters.

- To obtain the response of passive energy devices like friction and MR damper subjected to sinusoidal and different earthquake ground excitations, in order to characterize them.

- Consider three storey shear building and obtain damping matrix. Also, obtain uncontrolled response of the building under various earthquake excitations.

- Obtain seismic response of a three story shear building attached with passive devices like Friction and MR dampers subjected to various earthquake excitations, and extract the response quantities like displacement, velocity, acceleration, and inter storey drift for controlled building using numerical method through MATLAB.

- Analyze results obtain for uncontrolled building and compare with results of controlled building.

1.4 Scope of Work

Following is the scope of work:

- Carry out extensive literature review on implementation of passive and semi active devices for structural control of the building.
- Study, in detail, various mathematical models used for various passive and semi active energy dissipation devices.
- Compile various types of earthquake ground motion acceleration history data.
- Response characterization of damper under sinusoidal and random excitation.
- Discrete(lumped mass) model formulation of the building.
- Formulation and solution of equation of motion for building with and without passive and semi active energy dissipation devices using numerical method like Newmark-Beta and Runge Kutta through MATLAB.
- Extract response quantities like interstorey drift, displacement, velocity, acceleration, damper force etc.

1.5 Organization of Report

The Major Project is divided into eight chapters. They are as follows:

Chapter 2 deals with the details of literature review of various technical papers. It mainly focuses on the mathematical model, behavior and properties of different passive energy dissipation devices.

Chapter 3 consists study and characterization of passive devices. like friction and MR damper. Also it deals with the simulation of damper responses for friction and MR damper under sinusoidal and random excitations. Various earthquake excitations used to obtain damper responses are El Centro(1940), Loma Prieta (1989), Northridge (1994), and kobe (1995).

Chapter 4 includes Formulation and solution of equation of motion for building with and without passive devices using Newmark-Beta method under the four different excitations through MATLAB. Extraction of the response quantities for uncontrolled building like inter storey drift, displacement, velocity, acceleration and damping force.

Chapter 5 includes the shear building equipped with friction damper using Newmark-Beta method under four different earthquake excitations through MATLAB. Design of Friction damper is carried out for value of required damping force. Extraction of the response quantities like inter storey drift, displacement, velocity, acceleration and damping force are obtained.

Chapter 6 includes the shear building response by adding MR damper using Newmark-Beta method under the four different earthquake excitations through MATLAB. Design of MR damper and parametric study are carried out for value of required damping force. Extraction of the response quantities like inter storey drift, displacement, velocity, acceleration and damping force are obtained.

Chapter 7 includes the comparison of different passive devices for their response quantities.

Chapter 8 includes the summary of the study, conclusions and future scope of work.

Chapter 2

Literature Survey

2.1 General

Design for strength alone does not necessarily ensure that the building will respond dynamically in such a way that the comfort and safety of the occupants is maintained. For example, during the 1989 Loma Prieta earthquake, a 47-story.Building in San Francisco experienced peak accelerations of about 0.1% g in the basement and 0.45% g on the top floor, which indicates that harmful accelerations in the upper stories can result from strong ground accelerations.In fact, the requirements for strength and for safety can be conflicting. Thus, alternate means of increasing the resistance of a structure while maintaining desirable dynamic properties, based on the use of various active, semiactive, passive, and hybrid control schemes, offers great promise. This literature review provides glimpse of research related to energy dissipating devices.

2.2 Active Structural Control System

Active control strategies have been developed as one means by which to minimize the effects of these environmental loads (Soong,[1]; Housner and Masri,[11]). Active control systems operate by using external energy supplied by actuators to impart forces on the structure. The appropriate control action is determined based on measurements of the structural responses. For approximately two decades, researchers have investigated the possibility of using active control methods to improve upon passive approaches to reduce structural responses.

A variety of active control mechanisms have been suggested. These mechanisms include the active tendon system (Roorda,[19]; Abdel-Rohman and Leipholz,[2]), the active bracing system (Reinhorn,et al.,[17]), the active tuned mass damper/driver (Abdel-Rohman and Leipholz [2]; Chang and Soong [5]), and the active aerodynamic appendage mechanism (Soong and Skinner,[22]).

To evaluate the effectiveness of active structural control systems for earthquake hazard mitigation, the National Center for Earthquake Engineering Research (NCEER) has conducted extensive experiments on scale models of buildings. (Chung, et al . [7]) applied linear quadratic regulator theory to a SDOF structure equipped with an active tendon system and later extended this work to a three degree-of-freedom structure in Chung, et al . (1988) [7]. Reinhorn, et al .[18] also applied active control algorithms to a six-story model structure.

The first implementation of an active control system to a full-scale building was the Kyobashi Seiwa building in 1989 (Kobori 1994; Sakamoto, et al ., 1994) [12], as shown in figure 2.1. Two active mass drivers were installed on the top floor to reduce structural vibrations due to moderate earthquakes and strong winds, and to increase the comfort level of the buildings occupants. A primary AMD (4 tons) was employed to control the lateral motion and the secondary AMD (1 ton) controls the torsional motion.Active and hybrid structural control systems have subsequently been installed in over twenty buildings and utilized during the construction of more than ten bridges.

Even though a large amount of analytical and experimental research has been conducted in the last twenty years, and a number of full-scale structures in Japan have been equipped with active control systems, there are no full-scale, active control implementations in the U.S. This is partially due to the lack of standardized analysis and testing procedures for the control systems and devices. Moreover, the U.S. construction industry appears to be conservative and reluctant to employ new technologies. Before active control can gain general acceptance, a number of challenges must be addressed. According to Fujino et al ., [10], these challenges include: (i) reduction of

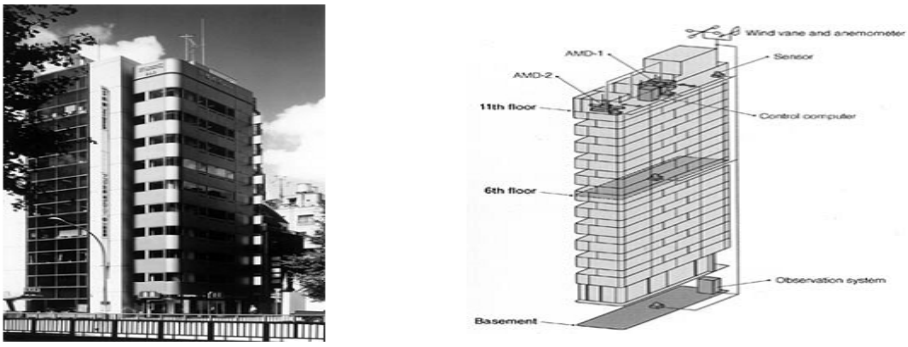

Figure 2.1: Kyobashi Seiwa Building with an AMD System.

capital cost and maintenance, (ii) eliminating reliance on external power, (iii) increasing system reliability and robustness, and (iv) gaining acceptance of nontraditional technology.

Although a number of questions still exist regarding the application of active control systems to civil engineering structures, the future is promising. Hybrid and semi-active control strategies appear to have the potential to address a number of the challenges to this technology. The following sections discuss some of the hybrid control systems, which are more mature, and recently proposed semi-active control systems, employing devices that potentially offer the reliability of passive devices, yet maintain the versatility and adaptability of fully active systems.

2.3 Hybrid Structural Control System

Hybrid control strategies have been investigated by many researchers to exploit their potential to increase the overall reliability and efficiency of the controlled structure (Soong and Reinhorn, [21]). A hybrid control system is typically defined as one which employs a combination of two or more passive or active devices. Because multiple control devices are operating, hybrid control systems can alleviate some of the restrictions and limitations that exist when each system is acting alone. Thus, higher levels of performance may be achievable. Additionally, the resulting hybrid control system can be more reliable than a fully active system, although it is also often more complicated. Research in the area of hybrid control systems has focused on two classifications of systems: i) hybrid mass damper systems, and ii) active base isolation.

The hybrid mass damper (HMD) is the most common control device employed in full-scale civil engineering applications. The HMD is a combination of a tuned mass damper (TMD) and an active control actuator. The ability of this device to reduce structural responses relies mainly on the natural motion of the TMD. The forces from the control actuator are employed to increase the efficiency of the HMD and to increase its robustness to changes in the dynamic characteristics of the structure. The energy and forces required to operate a typical HMD are far less than those associated with an fully active mass driver system of comparable performance. Figure 2.2 shows

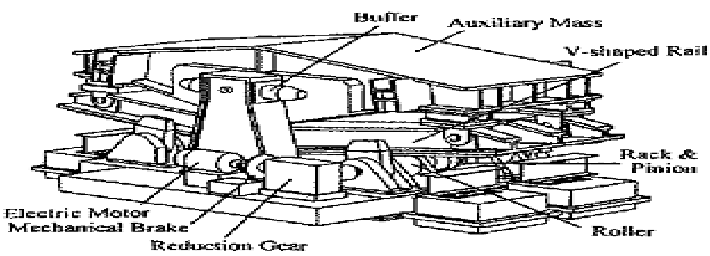

Figure 2.2: V-Shaped Hybrid Mass Damper.

an extension of the arch-shaped HMD, the V-shaped HMD (Koike, et al ., [13]), which has the advantage of an easily adjustable fundamental period. Three of these devices were installed in the Shinjuku Park Tower, the largest, in terms of square footage, building in Japan. Two multi-step pendulum HMDs (Yamazaki, et al ., 1992; Yamazaki, et al .,[20]) have been developed and installed in the Yokahoma Land-mark Tower, one of the tallest building in Japan.

2.4 Semi-Active Structural Control System

Semi-active control devices have received a great deal of attention in recent years because they offer the adaptability of active control devices without requiring the associated large power sources. In fact, many can operate on battery power, which is critical during seismic events when the main power source to the structure may fail. According to presently accepted definitions, a semi-active control device is one that cannot increase the mechanical energy in the controlled system (i.e., including both the structure and the device), but has properties which can be dynamically varied to optimally reduce the responses of a structural system.

Therefore, in contrast to active control devices, semi-active control devices do not have the potential to destabilize the structural system (in the bounded input/bounded output sense). Preliminary studies indicate that appropriately implemented semi-active systems perform significantly better than passive devices and have the potential to achieve, or even surpass, the performance of fully active systems, thus allowing for the possibility of effective response reduction during a wide array of dynamic loading conditions.

Examples of such devices include variable-orifice fluid dampers, controllable friction devices, variable stiffness devices, controllable liquid dampers and controllable fluid dampers. Various semi-active devices have been proposed which utilize forces generated by surface friction to dissipate vibratory energy in a structural system. Akbay and Aktan [3] proposed variable friction devices which consists of a friction shaft which is rigidly connected to the structural bracing. The force at the frictional interface was adjusted to allow controlled slippage.Through analytical studies, the ability of these semi-active devices to reduce the interstory drifts of a seismically excited structure was investigated. In addition, a semi-active friction-controllable fluid bearing has been employed in parallel with a seismic isolation system. Another class of semi-active devices uses controllable fluids. The advantage of controllable fluid devices is that they contain no moving parts other than the piston, which makes them very reliable. Figure 2.3 shows schematic of controllable fluid damper although a variety of designs have been investigated. Two fluids that are viable contenders for

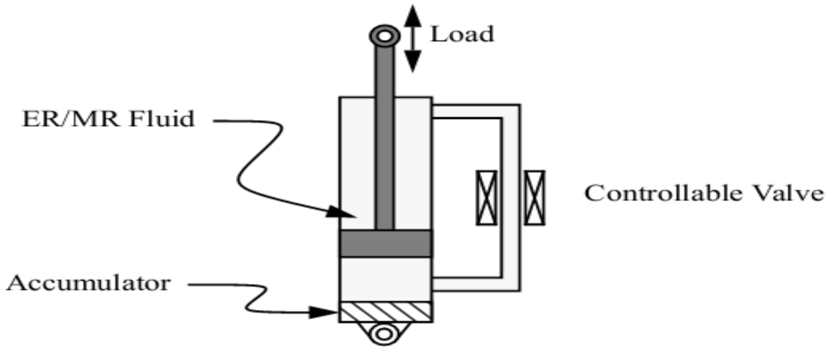

Figure 2.3: Schematic of a Controllable Fluid Damper.

development of controllable dampers are: (i) electrorheological (ER) fluids and (ii) magnetorheological (MR) fluids. The essential characteristic of controllable fluids is their ability to reversibly change from a free-flow-ing, linear viscous fluid to a semi-solid with a controllable yield strength in milliseconds when exposed to an electric (for ER fluids) or magnetic (for MR fluids) field. Although the discovery of both ER and MR fluids dates back to the late 1940s, research programs have to date concentrated primarily on ER fluids. A number of ER fluid dampers have recently been developed, modeled, and tested for civil engineering applications(McClamroch and Gavin, [14]). Recently developed MR fluids appear to be an attractive alternative to ER fluids for use in controllable fluid dampers (Carlson, et al. [4]). MR fluids typically consist of micron-sized, magnetically polarizable particles dispersed in a carrier medium such as mineral or silicone oil. When a magnetic field is applied to the fluid, particle chains form, and the fluid becomes a semi-solid and exhibits viscoplastic behavior similar to that of an ER fluid. Transition to rheological equilibrium can be achieved in a few milliseconds, allow-ing construction of devices with high bandwidth. Additionally, Carlson and Weiss [4] indicated that the achievable yield stress of an MR fluid is an order of magnitude greater than its ER counterpart and that MR fluids can operate at temperatures from 40 to 150^0 C with only slight variations in the yield stress.

Moreover, MR fluids are not sensitive to impurities such as are commonly encountered during manufacturing and usage, and little particle/carrier fluid separation takes place in MR fluids under common flow conditions. Further, a wider choice of additives (surfactant, dispersants, friction modifiers, anti-wear agents, etc.) can generally be used with MR fluids to enhance stability, seal life, bearing life, etc, since electro-chemistry does not affect the magneto-polarization mechanism. The MR fluid can be readily controlled with a low voltage (e.g., 1224V), current-driven power supply outputting only 12 amps.

The future of MR devices for civil engineering applications appears to be quite bright (Spencer, et al ., 1996ad; Dyke, et al ., 1996cf). Because all of these semi-active devices are intrinsically nonlinear, one of the main challenges is to develop control strategies that can optimally reduce structural responses. Various nonlinear control strategies have been developed to take advantage of the particular characteristics of the semi-active devices, including bang-bang control (McClamroch and Gavin, [14]), clipped-optimal control (Dyke, et al ., [9])

2.5 Passive Structural Control System

Benefit-cost analysis approach suggests performance-based design for most modern buildings by (Avtar Pall and R. Tina Pall et al. [16]). The conventional structural systems are highly unlikely to provide adequate performance in the event of a major earthquake. With the emergence of Pall Friction Dampers, it has now become economically feasible to design high performance structures. Their low cost and maintenance free characteristics suggest wide application for new construction as well as for retrofit of existing buildings. Public sectors, private sectors, developers and developing countries are all benefiting from this technology. They have been used for the seismic protection of more than 80 major building projects, including the Boeing Commercial Airplane Factory at Everett, WA - the world's largest building in volume presented a concise point of departure for researchers and practitioners alike wishing to assess the current state of the art in the control and monitoring of civil engineering structures, and provides a link between structural control and other fields of control theory.

A new concept of aseismic design for steel framed buildings is proposed. By providing sliding friction devices in the bracing system of the framed buildings, their earthquake resistance and damage control potential can be considerably enhanced. Figure 2.4 shows typical arrangement of friction damper. During severe earthquake excitations,

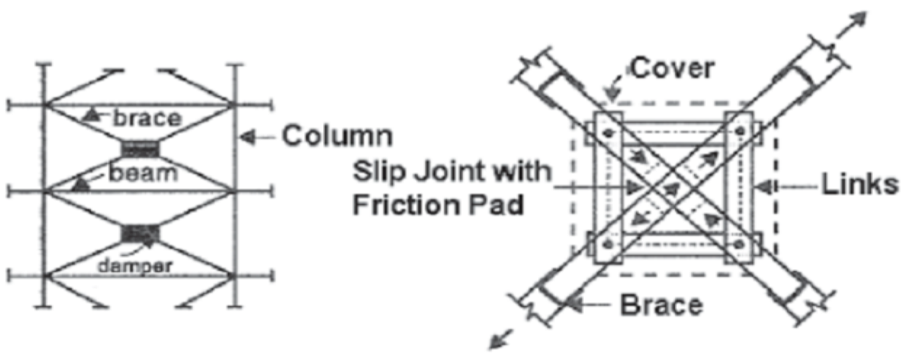

Figure 2.4: X Braced Friction Damper.

the friction device slips and a large portion of the vibrational energy is dissipated mechanically in friction rather than inelastic yielding of the main structural components. Results of inelastic time history dynamic analysis show superior performance of the friction damped braced steel frames when compared with the computed responses of other structural framing systems. The proposed friction devices act, in effect, both as safety valves and structural dampers. The device may also be conveniently incorporated in existing framed buildings to upgrade their earthquake resistance.

2.6 Summary

In this chapter, review of relevant literature is carried out. The review of literature includes, mathematical modeling, hysteresis behavior and properties of various passive dampers. Basic concept of analysis of damper added structure are carried out.

Chapter 3

Passive Control Systems

3.1 Introduction

Dynamic load produces vibration in the structure which causes the damage or collapse of the structure. A large amount of energy is imparted into structure during these vibrations. To reduce these vibrations it becomes important for the structure to absorb or dissipate energy. Research is under way to reduce the response of the structures resulting due to dynamic loading. A widely considered strategy consists of incorporating external elements to the structure to control its dynamic response. The branch of Structural Engineering that deals with such concepts is called Structural Control.

The function of seismic passive energy dissipation system is to reduce structural response due to earthquake, wind and other dynamic loads. Passive control system develops control forces at the point of attachment of the system. The power needed to generate these forces is provided by the motion of the points of attachment during dynamic excitation. Passive energy dissipation systems encompass a range of materials and devices for enhancing damping, stiffness and strength, and can be used both for natural hazard mitigation and for rehabilitation of aging or deficient structures.

In recent years, serious efforts have been undertaken to develop the concept of energy dissipation or supplemental damping into a workable technology and a number of such devices have been installed in structures throughout the world [8, 23]. In general, they are all characterized by a capability to enhance energy dissipation in the structural systems to which they are installed. This may be achieved either by conversion of kinetic energy to heat, or by transferring of energy among vibrating modes. The first method includes devices that operate on principles such as frictional sliding, yielding of metals, phase transformation in metals, deformation of viscoelastic solids or fluids, and fluid orificing. The latter method includes supplemental oscillators, which act as dynamic vibration absorbers.

3.2 Classification of Energy Dissipation Devices

Passive energy dissipaters may be simply classified as,

1) Displacement Dependent Devices

- Friction Damper
- Metallic Damper

2) Velocity Dependent Devices

- Viscous Damper
- Solid and Fluid Viscoelastic Damper

3) Dynamic Vibration Absorber

- Shape-Memory Alloys
- Tune Mass or Tune Liquid Oscillator Type Damper

3.2.1 Displacement Dependent Devices

Displacement-dependent devices dissipate energy through sliding friction, like friction dampers, or through the inelastic behavior of the damper elements, like metallic dampers because their energy dissipation depends primarily on relative displacements within the device and not on their relative velocities. A variety of hysteretic devices has been proposed and developed to enhance structural safety. The majority of these devices generate rectangular hysteresis loop. This indicates that behavior of friction dampers is close to that of coulomb friction. The simplest models of hysteretic behavior involve algebraic relation between force and displacement. Hence, hysteretic devices are often called displacement dependant.

3.2.2 Velocity Dependent Devices

Velocity dependent devices like viscous and VE elastic dampers dissipate energy through deformation of VE polymers, deformation of viscous fluids, or fluid orificing. Their energy dissipation depends on both relative displacements and relative velocities within the device. Velocity-dependent devices provide damping and stiffness to the structures while displacement dependent devices provides stiffness and energy dissipations takes place under moderate ground motions only.

3.2.3 Dynamic Vibration Absorber

A dynamic vibration absorber (DVA) is a typical example of a passive controller. It consists of an auxiliary mass-spring system which tends to neutralize the vibration of a structure to which it is attached. The basic principle of operation is vibration out of phase with the vibration of such structure, thereby applying a counteracting force. An absorber is only effective at its natural frequency which must be tuned to coincide with the forcing frequency. The example of DVA are shape memory alloy and tune mass damper. Tune mass damper consists of a secondary mass with properly tuned spring and damping elements, providing a frequency-dependent hysteresis that increases damping in the structure.

Table 3.1: Passive Devices and its Principle of Operation

Type	Device	Principle of operation
Hysteretic	Metallic yielding	Yielding of metals
	Friction	Frictional sliding
VE	VE solids	Deformations of VE polymers
	Viscous and VE fluids	Deformation of viscous fluid

Table 3.1 shows the supplemental energy dissipation devices and its principle of operation. Arrangement of viscoelastic damping system in building structure is shown in Figure 3.1.

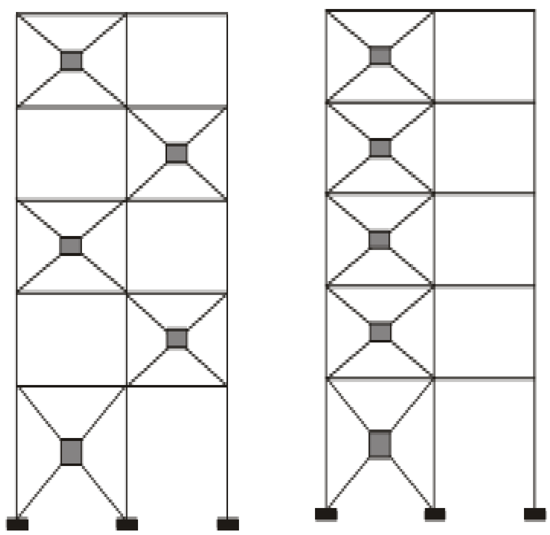

Figure 3.1: Damper Placement within Structure

In the next section, major focus is to study effectiveness of the Friction damper and MR Damper are consider in mitigating the responses. However, before that characterization of such damper is essential, in order to understand the dynamics of the dampers. Therefore, damper are subjected to sinusoidal motion and four different characteristics of earthquake motions. The earthquake events used in characterization are El Centro (1940), Loma Prieta (1989), Northridge (1994), and Kobe (1995) time histories.

3.3 Friction Damper

These devices rely on the resistance developed between two solid interfaces sliding relative to one another.During severe seismic excitations, the device slips at a predetermined load, providing the desired energy dissipation by friction while at the same time shifting the structural fundamental mode away from the earthquake resonant frequency. Friction dampers are not susceptible to thermal effects, have a reliable performance and possess a stable hysteretic behavior for a large number of cycles under a wide range of excitation conditions.

In mid 1970's, Pall Friction Dampers were pioneered for the seismic control of build-

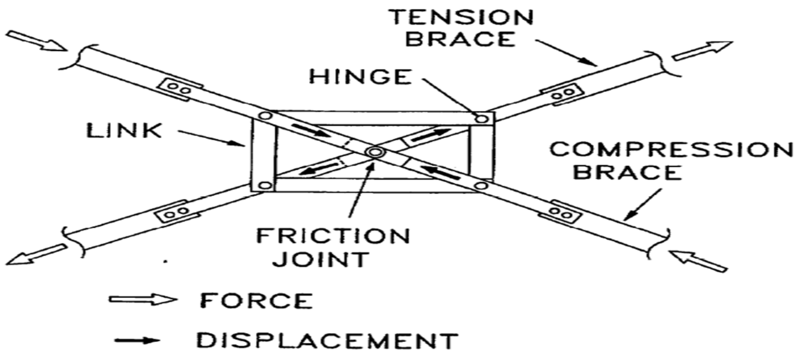

Figure 3.2: Friction Damper

ings. Pall Friction Dampers significantly reduce the initial cost of construction while dramatically increasing the earthquake resistance against damage. Developing a reliable friction is very difficult and tricky. Over a period of more than a decade of research and development, the common problems in friction were successfully overcome by using specially treated surfaces and a unique manufacturing process. Over the years, Pall Dynamics has earned an international reputation for excellence and is a world leader in friction dampers for seismic control of buildings.

Pall Friction Dampers are well recognized and accepted by the building codes in Canada, the U.S and many other countries.Pall Friction Dampers are foolproof in construction. Basically, these consist of series of steel plates, which are specially treated to develop very reliable friction. These plates are clamped together and allowed to slip at a predetermined load.Their performance is independent of velocity and hence exerts constant force for all future earthquakes, design-based earthquake (DBE) or maximum credible earthquake (MCE).Pall Friction Dampers are passive energy dissipation devices and, therefore, need no energy source other than earthquake to operate it. They do not require any repair or replacement after the earthquake and are always ready to do their job. Figure 3.2 shows forces and deflection in friction damper.If a given structure requires certain total macroscopic damping, to implement this damping will involve dividing the total damping by the number of dampers used. The end result is a maximum force and damping function for each individual damper.

3.3.1 Mathematical Model and Behavior

Different mathematical models have been proposed in literature to predict the behavior of friction devices. Figure 3.2 shows a simple friction damper, in which friction element is connected. However, for typical structural applications the friction damper can be modeled as a simple friction element in which the velocity is directly proportional as given in Figure 3.3.

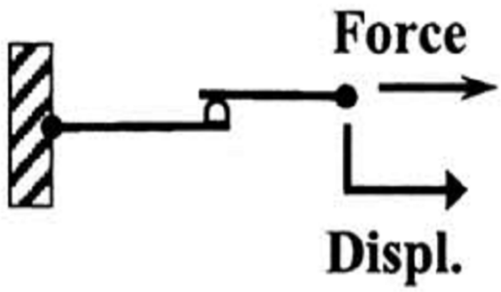

Figure 3.3: Simple Physical Model for Friction Damper

The force in the friction damper may be expressed in equation 3.1,

$$F = \mu N sgn(\dot{u}) \tag{3.1}$$

Where, μ is the coefficient of dynamic and static friction , N is the Normal force at the sliding surface, $\dot{u}$ is the relative velocity between each end of the device, and sgn is the signum function that, defines the sign of the relative velocity term.

$$E_D = 4P_y(d_0 - d_y) \tag{3.2}$$

The area contained within the hysteretic loop present in figure 3.4, measures the energy dissipated per cycle in the friction damper.

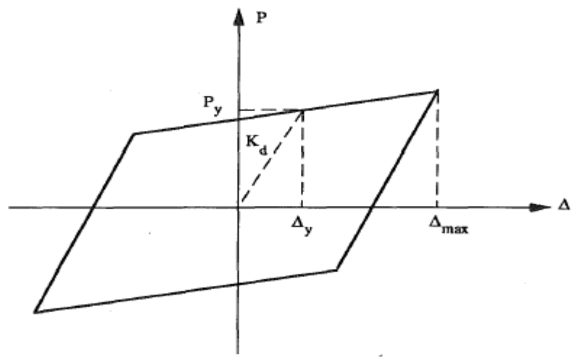

Figure 3.4: Hysteresis Loop for Friction Damper [11]

3.3.2 Response of Friction Damper

The cyclic response of friction damper is dependent on the displacement of motion, may be dependent on the amplitude and frequency of motion; and is generally independent on the operating temperature. Friction device may be modeled using friction element, i.e. coloumb Model.

3.3.2.1 Response of Damper Subjected to Sinusoidal Input

In the present study of characterization of friction damper is considered as given in literature. The plots of Force Vs Time, Force Vs Displacement, and Force Vs Velocity of viscous damper subjected to sinusoidal excitations with frequency of 1 to 5 Hz and value of amplitude ('a' = 50 mm) and frictional force is 30 N is same for all the response quantities are shown in Figure 3.5. Force time history as shown in Figure

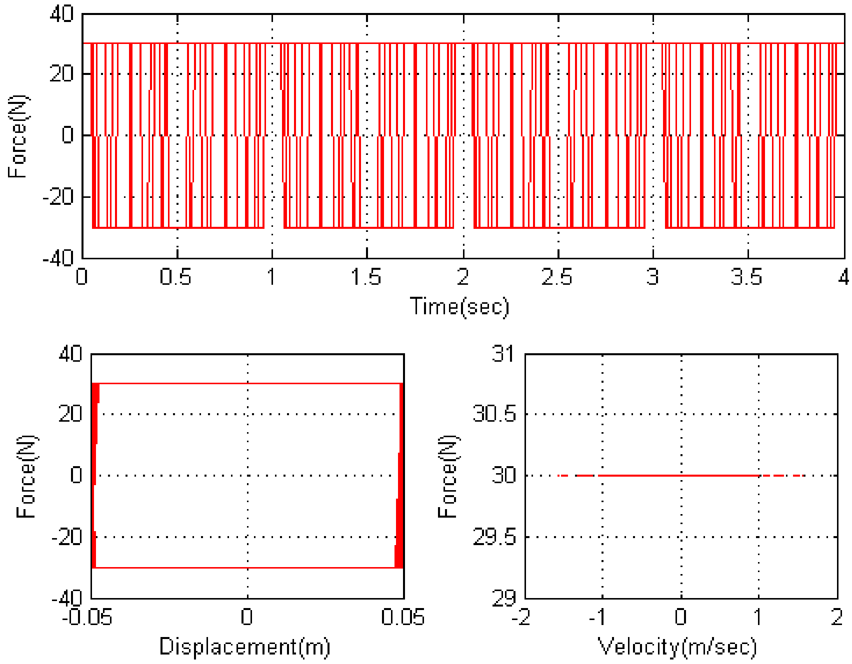

Figure 3.5: Response For Different Amplitude of Motion

3.5. It is clear from force-displacement plot that curve is rectangular. The energy dissipates is equal to area under an oval. It is evident from Figure 3.5 that force-velocity plot of friction damper is linear in nature and it is independent of velocity.

3.3.2.2 Response of Damper Subjected to Earthquake Input

In general, earthquakes have different response quantities such as Peak Ground Acceleration (PGA), Peak Ground Velocity (PGV), Peak Ground Displacement (PGD), duration of strong motion and ranges of dominant frequencies; hence they have different influence on the structures. In order to ensure that the chosen mitigation procedure is effective under different types of excitations, four well-known earthquake records are used in this study. The time history data was taken from "Pacific Earthquake Engineering Research Institute" (PEER). The earthquake time history records, which are selected for this study to investigate the dynamic response of viscous damper models are summarized in Table 3.2.

Plot of acceleration with respect to time for different earthquake time histories are shown in Figure 3.6. In this study same properties of friction damper are considered as used in case of damper subjected to sinusoidal input. In simulation of friction damper under different earthquake excitations, input of earthquake ground velocity is used. Force Vs Time, Force Vs Displacement, and Force Vs Velocity relationship to understand the behavior of friction damper under earthquake excitations are given in Figure 3.7 to Figure 3.10.

Table 3.2: Time History Data for Various Earthquakes

Earthquake	Year	PGA(g)	PGV(cm/sec^2)	PGD(cm)	Damping
El centro	1940	0.3129	43.8	18.3	0.05
Kobe	1995	0.6936	37.3	9.52	0.05
Loma prieta	1989	0.6437	94.8	41.18	0.05
Northridge	1994	1.585	103.9	23.8	0.05

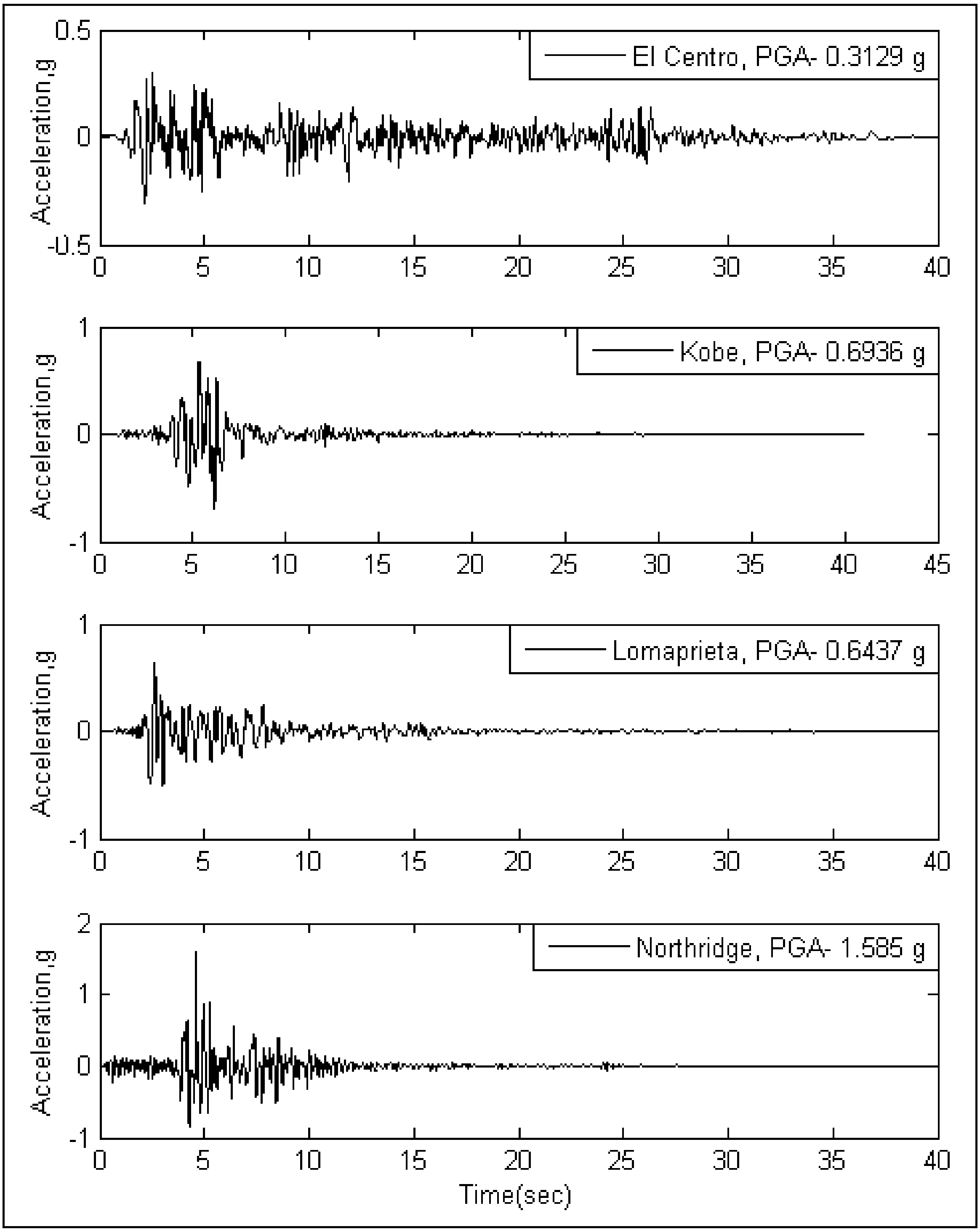

Figure 3.6: Earthquake Time History

Force time history of friction damper under the El Centro earthquake excitations is shown in Figure 3.7. It indicates that, resisting force value of viscous damper are varying with respect to time. The value 30 N, 0.133 m, and 0.23 m/sec are the maximum damper force, displacement and velocity under the EL Centro excitations respectively. From, force time history of El Centro excitation, it is reveals that strong motion duration is elapsed between (2-5) sec and (9-22) sec observed. In figure 3.7, Force Vs Displacement plot shows that area within hysteresis loop gives energy dissipation of friction damper under the El Centro Excitation. Force Vs Velocity plot shows the damper force is linear in nature.

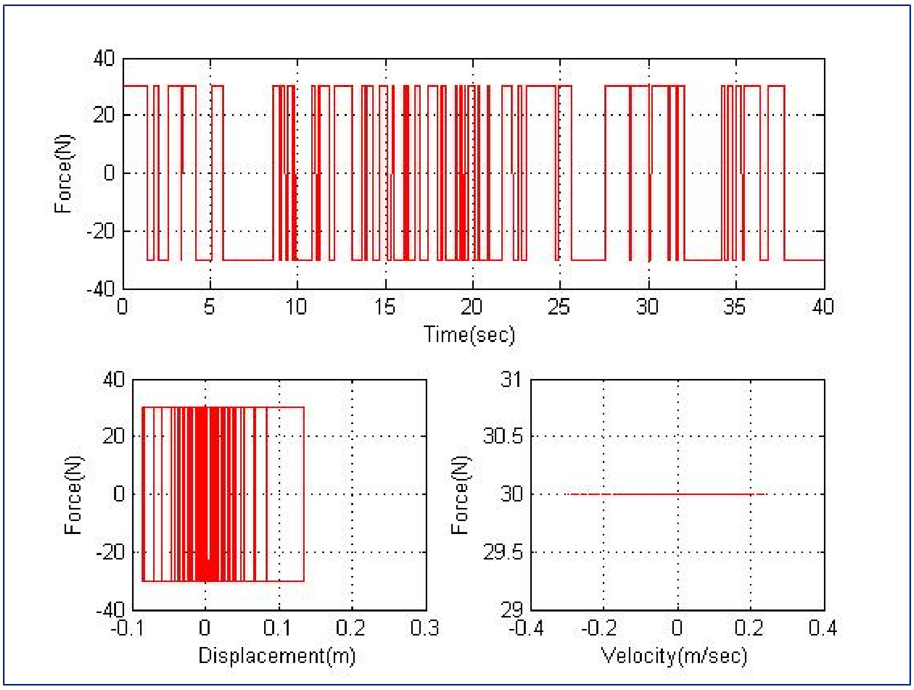

Figure 3.7: Response under 0.3129 g El Centro Earthquake

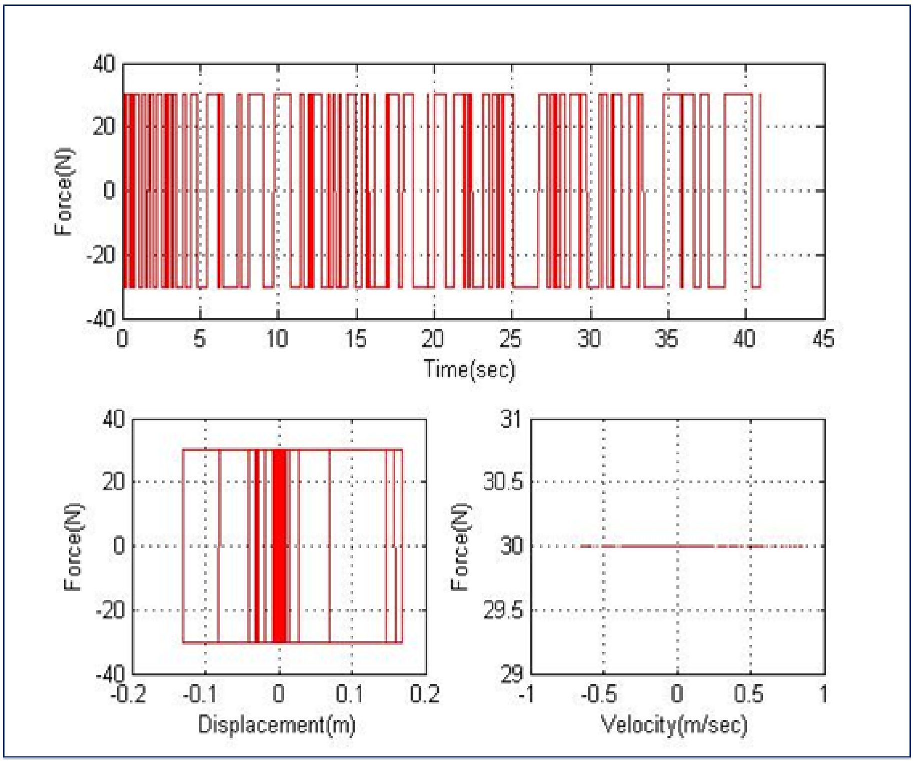

Figure 3.8: Response under 0.6936 g Kobe Earthquake

Force time history of friction damper under the Kobe earthquake excitations is shown in Figure 3.8. It indicates that, resisting force value of friction damper are varying with respect to time. The value 30 N, 0.1675 m, and 0.852 m/sec are the maximum damper force, displacement and velocity under the Kobe excitations respectively. In figure 3.8, Force Vs Displacement plot shows that area within hysteresis loop gives energy dissipation of friction damper under the Kobe Excitation, there is less number of cycles produces as compare to El Centro earthquake. Force Vs Velocity plot shows the damper force is linear in nature. Force time history as shown in Figure 3.9 indicates that damper force are varying with respect to time under Loma Prieta earthquake. The value 30 N, 0.108 m, and 0.5518 m/sec are the maximum damper force, displacement and velocity under the Loma Prieta excitations respectively. Force Vs Displacement plot of friction damper for Loma Prieta earthquake shows that area within hysteresis loop gives energy dissipation of friction damper. Figure 3.10 shows the Force Vs Time, Force Vs Displacement, and Force Vs Velocity

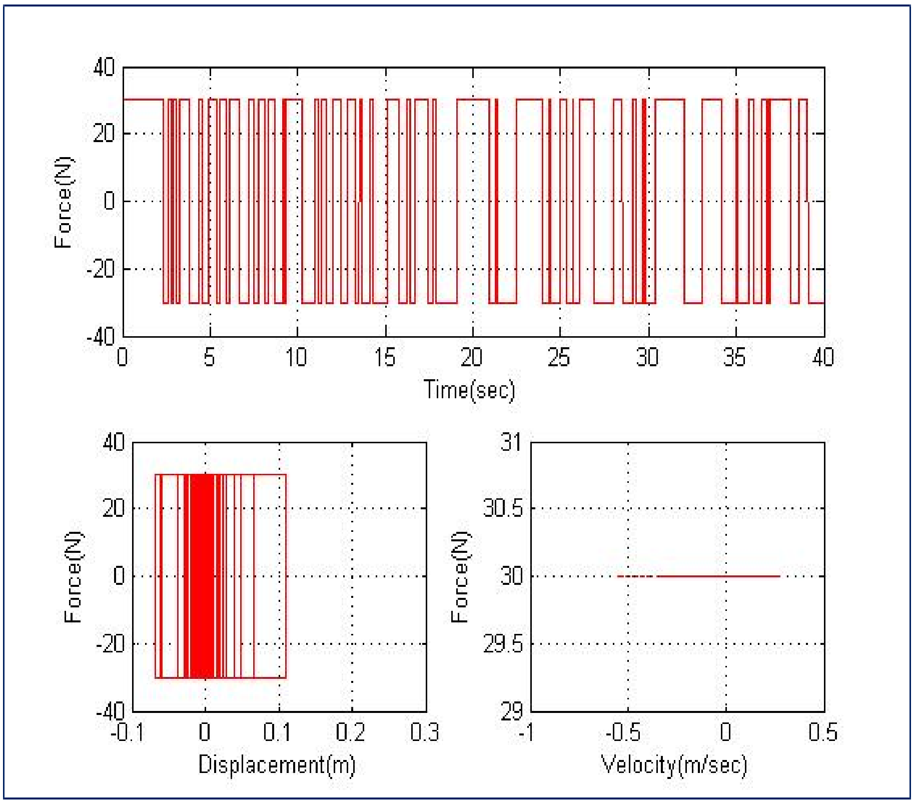

Figure 3.9: Response under 0.6437 g Loma Prieta Earthquake

plots of friction damper response under the Northridge Earthquake. The value 30 N, 0.0606 m, and 0.557 m/sec are the maximum damper force, displacement and velocity under the Loma Prieta excitations respectively. In this figure total area under the hysteresis loops are shown, which is indicates total energy dissipates under the Northridge earthquake. Damper force 30 N that is same for all earthquake.

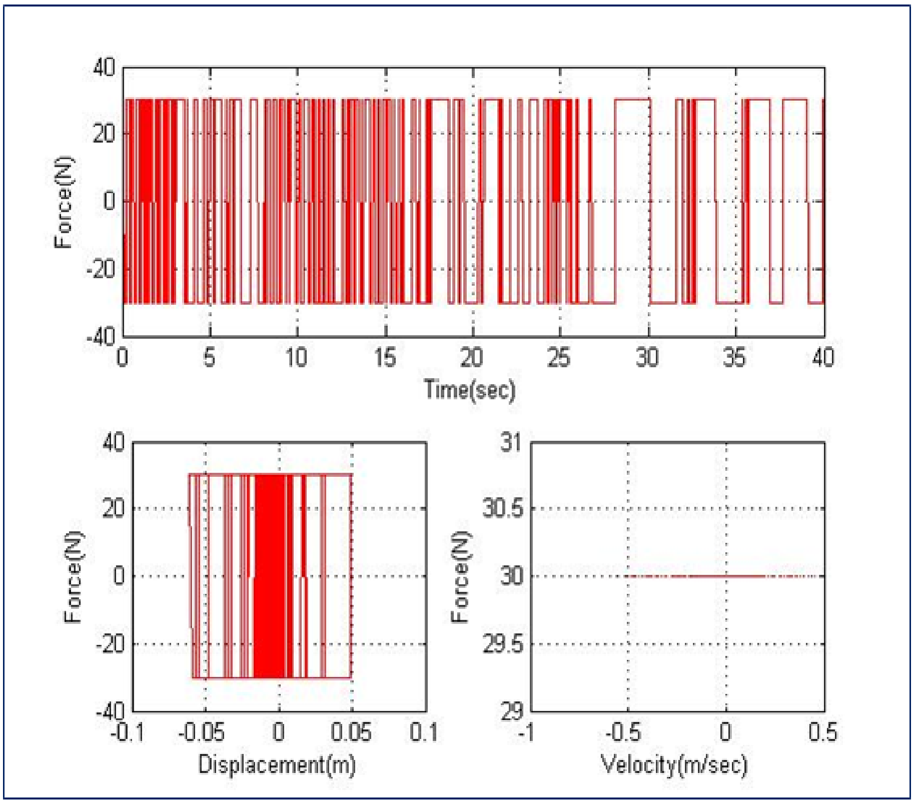

Figure 3.10: Response under 1.585 g Northridge Earthquake

3.4 Magneto - Rheological(MR) Damper

The magneto-rheological (MR) damper is one of the most promising new devices for structural vibration reduction. MR dampers are used with several control strategies in order to reduce the structural response. The concept of employing structural control to minimize structural vibration was proposed in the 1970s.There has been a great deal of interest in recent years in use of magneto-rheological(MR) dampers for semi-active structural control. The advantages of using such devices include low power requirements, high reliability, ensured stability of the control system, and higher force capacities in comparison to other types of damping devices.Semi-active control systems combine the features of active and passive control to reduce the response of structures to various dynamic loadings. Semi-active control systems are a class of active control systems for which the external energy requirements are orders of magnitude smaller than typical active control systems.Typically, semi-active control devices do not add mechanical energy to the structural system (including the structure and the control actuators), therefore bounded-input bounded-output is guaranteed. Semi-active control devices are often viewed as controllable passive devices. A prototype magneto-rheological (MR) damper has been obtained from the Lord Corporation of Cary, North Carolina to evaluate the usefulness of MR devices in response reduction for civil engineering structures.

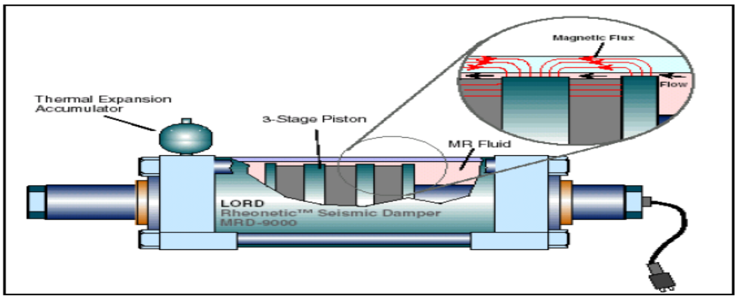

Figure 3.11: Magneto-Rheological (MR) Damper

MR fluids are the magnetic analogs of electro-rheological (ER) fluids which have also been considered for structural control applications. The essential characteristic of these controllable fluids is their ability to reversibly change from a free-flowing, linear, viscous fluid to a semi-solid in milliseconds when exposed to a magnetic (or electric in the case of ER fluids) field. Recently developed MR fluids have high strength, low viscosity, and low power requirements, are stable over a broad temperature range and are insensitive to impurities commonly introduced during manufacturing. Because there are no moving parts, other than the piston itself, damping devices that take advantage of controllable fluids are simpler and more reliable than semi-active dampers based on electromechanical devices.

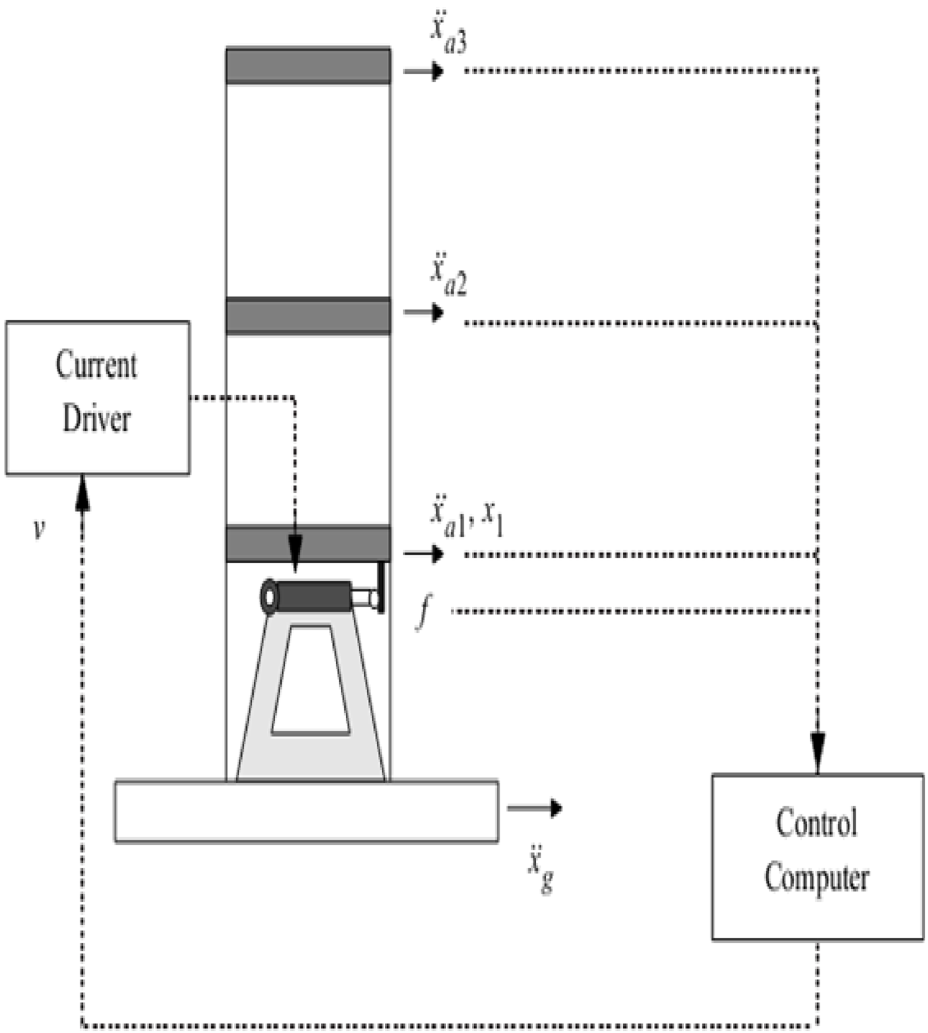

Figure 3.12: Placement of Magneto-Rheological (MR) Damper in building

Furthermore, the MR damper is expected to be quite inexpensive to build and operate, and preliminary tests indicate that it will be capable of generating the required forces for civil engineering applications. Figure 3.12 shows MR damper.

3.4.1 Mathematical Model and Behavior

Both nonparametric and parametric models have been considered to model the observed behavior of controllable fluid damper. The Bingham viscoplastic model. The Bingham viscoplastic model (Shames and Cozzarelli, 1992) is often used to describe the stress-strain behavior of MR (and ER) fluids. In this model, the plastic viscosity is defined as the slope of the measured shear stress versus shear strain rate data. Based on the Bingham model, Stanway, et al. (1985, 1987) proposed an idealized mechanical model, denoted the Bingham model, for the behavior of an ER damper. The Bingham model consists of a Coulomb friction element placed in parallel with a viscous damper, as shown in figure 3.13. In this model, for nonzero piston velocities,

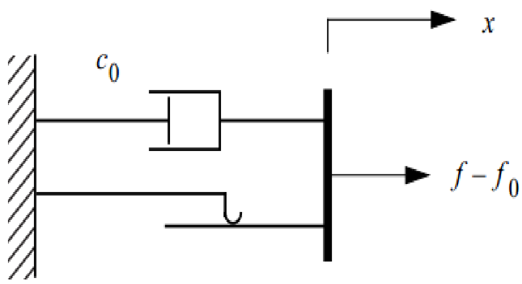

Figure 3.13: Bingham Model of a Controllable Fluid Damper

, the force generated by the device given by

$$F(t) = f_f sgn(x) + C(\dot{x}) + f_0 \tag{3.3}$$

where c0 is the damping coefficient and ff is the frictional force, which is related to the fluid yield stress. An offset in the force is included to account for the nonzero mean observed in the measured force due to the presence of the accumulator. Note that if at any point the velocity of the piston is zero, the force generated in the frictional element is equal to the applied force. To assess its ability to predict the behavior of the MR damper, the model in was fit to the 2.5 Hz sinusoidal response data shown

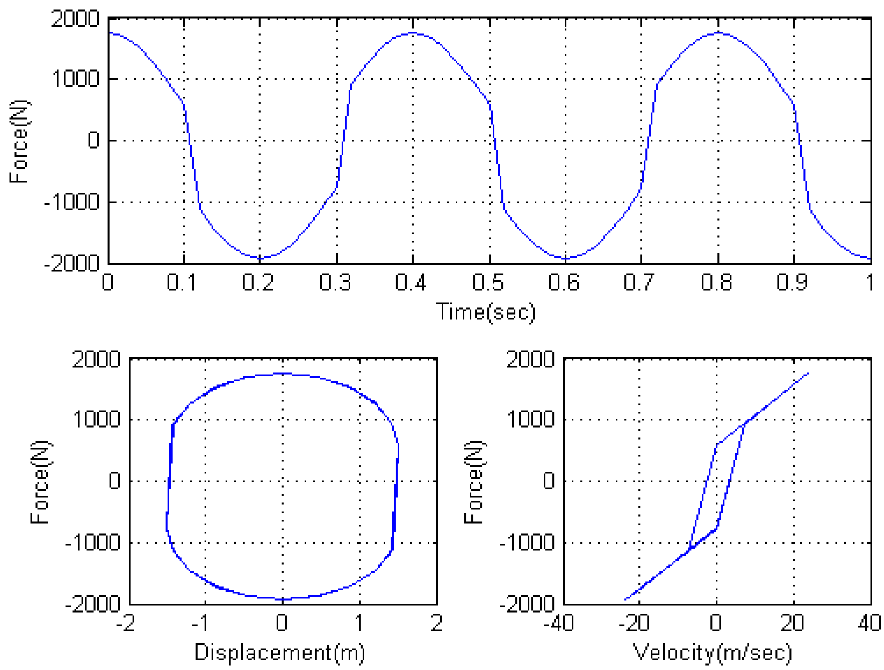

Figure 3.14: Response For Different Excitation of Frequency

in figure 3.14. For the case in which the command voltage to the current driver was a constant 1.5 V. The parameters chosen are ff=670 N, c_0 = 50 N sec/cm and f_0 = -95 N. Figure shows a response under 2.5 Hz sinusoidal response. In particular, this model does not exhibit the nonlinear force-velocity response observed in the data for the case when the acceleration and velocity have opposite signs. While this model may be adequate for response analysis, it is not adequate for control analysis. One model that is numerically tractable and has been used extensively for modeling hysteretic systems is the Bouc-Wen model. The Bouc-Wen model is Experimental Predicted extremely versatile and can exhibit a wide variety of hysteretic behavior. A schematic of this model is shown in figure 3.15. The force in this system is given by

$$f = c_0\dot{x}_d + k_0(d_0 - d_y) + \alpha z \tag{3.4}$$

where the evolutionary variable z is governed by

$$\dot{z} = -\gamma \dot{x_d} z z^{n-1} - \beta \dot{x_d} z^n + A\dot{x_d} \quad (3.5)$$

By adjusting the parameters of the model gamma, beta and A one can control the linearity in the unloading and the smoothness of the transition from the pre-yield to the post-yield region. In addition, the force f_0 due to the accumulator can be directly incorporated into this model as an initial deflection x_0 of the linear spring k_0. A set of parameters was determined to fit the response of the Bouc-Wen model to

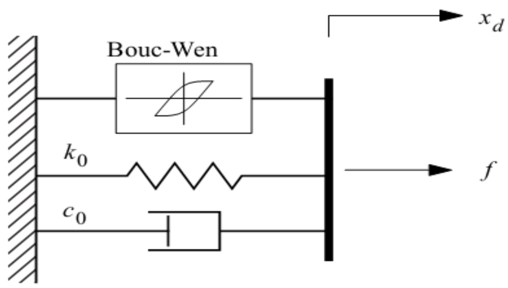

Figure 3.15: Bouc-Wen Model of a Controllable Fluid Damper

the experimentally measured response of the MR damper shown in Fig. 7.3 (2.5 Hz sinusoidal displacement and a constant applied voltage of 1.5V). The parameters for the model in eq 3.4 were chosen to be α=880 N/cm, c_0= 50 N sec/cm, k0=25 N/cm, $\gamma = 100\ cm^2$, $\beta = 100\ cm^2$ n=2, A=120 , and x0=3.8 cm. Response of Bouc-Wen model is shown in figure 3.16.

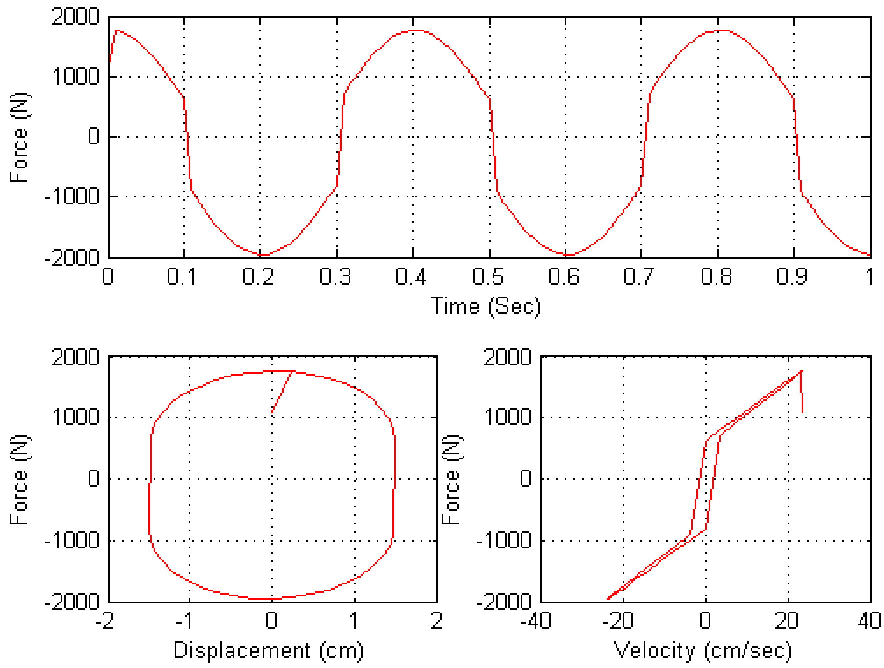

Figure 3.16: Response For Different Excitation of Frequency

The Bouc-Wen model predicts the force-displacement behavior of the damper well, and it possesses force-velocity behavior that more closely resembles the experimental data. However, similar to the Bingham model, the nonlinear force-velocity response of the Bouc-Wen model does not roll-off in the region where the acceleration and velocity have opposite signs and the magnitude of the velocities are small. To better predict the damper response in this region, a modified version of the system in figure 3.15 is proposed, as shown in figure 3.17. To obtain the governing equations for this model, consider only the upper section of the model. The forces on either side of the rigid bar are equivalent; there-fore,

$$c_1 \dot{y_d} = c_0(\dot{x_d} - \dot{y_d}) + k_0(d_0 - d_y) + \alpha z \tag{3.6}$$

where the evolutionary variable z is governed by

$$\dot{z} = -\gamma(\dot{x_d} - \dot{y_d}) z z^{n-1} - \beta(\dot{x_d} - \dot{y_d}) z^n + A(\dot{x_d} - \dot{y_d}) \tag{3.7}$$

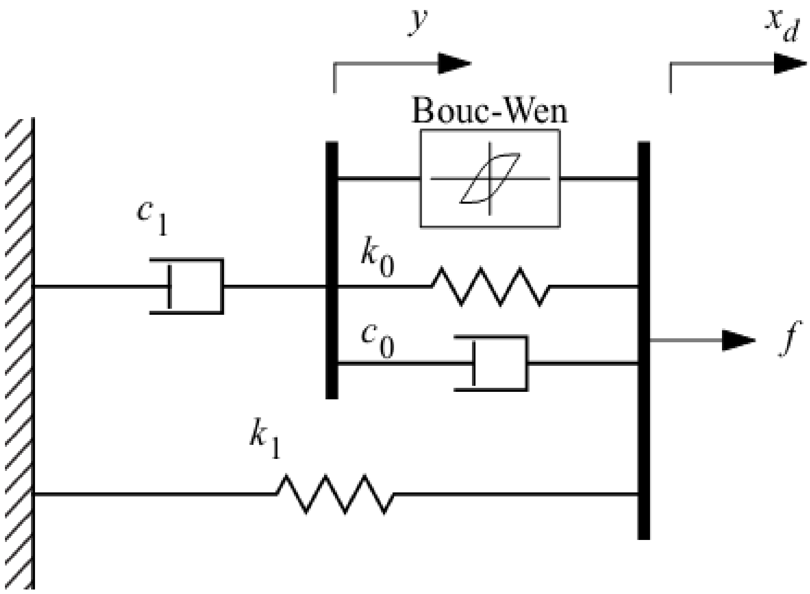

Figure 3.17: Proposed Mechanical Model of the MR Damper

Solving (3.7) for $\dot{y}_d$ results in

$$\dot{y} = (1/(c_0 + c_1))(c_0\dot{x_d} + k_0(d_0 - d_y) + \alpha z) \tag{3.8}$$

The total force generated by the system is then found by summing the forces in the upper and lower sections of the system in Figure 3.17, yielding

$$f = \alpha z + c_0(\dot{x_d} - \dot{y_d}) + k_0(x_d - y) + k_1(x_d - x_0) \tag{3.9}$$

From (3.7), the total force can also be written as

$$f = c_0\dot{y_d} + k_1(x_d - x_0) \tag{3.10}$$

In this model, the accumulator stiffness is represented by and the viscous damping observed at larger velocities is represented by . A dashpot, represented by , is included in the model to produce the roll-off that was observed in the experimental data at low velocities, is present to control the stiffness at large velocities, and is the initial displacement of spring associated with the nominal damper force due to the accumulator. The parameters for the model were chosen to be α = 963 N/cm, c_0 = 53 N sec/cm, k_0 = 14 N/cm, c_1 = 930 N sec/cm, k_1 = 5.4 N/cm, γ = 200 cm^{-2}, β = 200 cm^{-2},n = 2 ,A = 207 ,and x_0 = 18.9 cm, which fit the response of the proposed model to the 2.5 Hz data shown in Figure 3.18 for the case where the voltage to the current driver was 1.5 V. The proposed model for the damper predicts

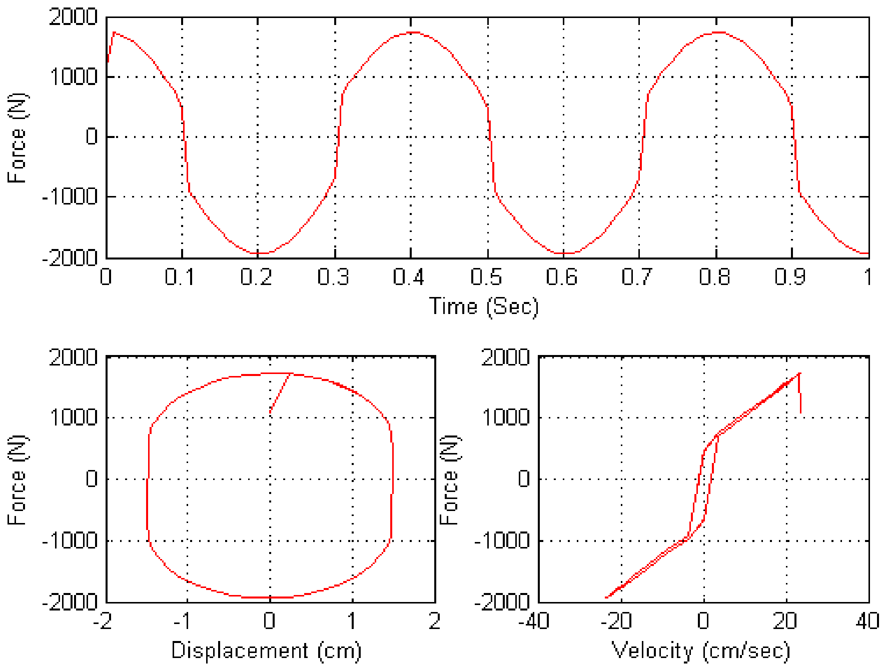

Figure 3.18: Response For Different Excitation of Frequency

the behavior of the damper very well in all regions, including in the region where the acceleration and velocity have opposite signs and the magnitude of the velocities are small. The response which are obtained is for constant voltage. All of the data that was examined previously has been based on the response of the MR damper when the applied voltage, and hence the magnetic field, was held at a constant level. However, optimal performance of a control system which utilizes this device is expected to be achieved when the magnetic field is continuously varied based on the measured response of the system to which it is attached. To use the damper in this way, a model

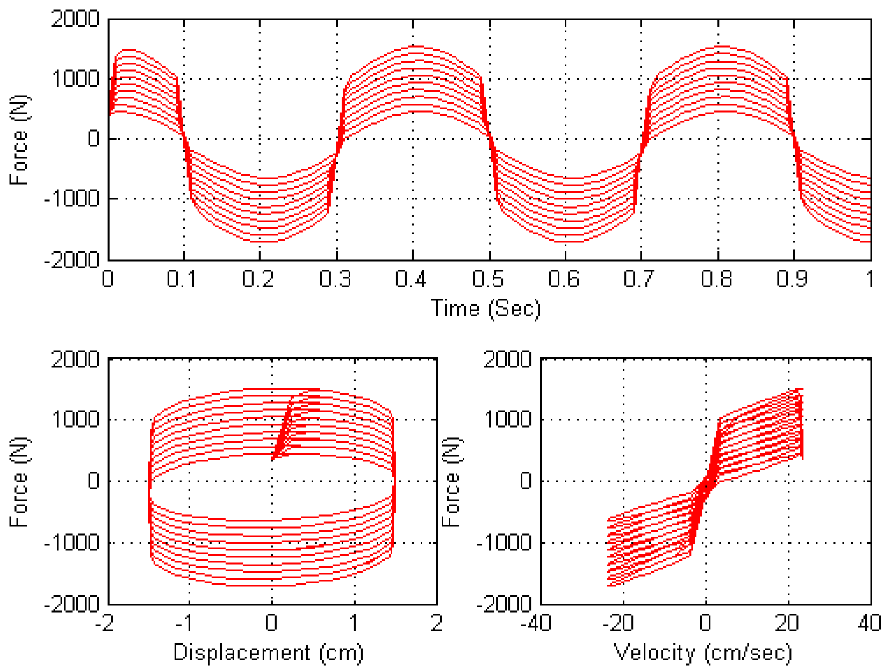

Figure 3.19: Response For Different Excitation of Voltage

must be developed which is capable of predicting the behavior of the MR damper for a fluctuating magnetic field. To determine a model that is valid for fluctuating magnetic fields, the functional dependence of the parameters on the applied voltage (or current) must be determined. Figure 3.19 shows as the voltage increases, the force required to yield the MR fluid in the damper increases and produces behavior associated with a plastic material in parallel with a viscous damper.

3.5 Summary

This chapter deals with the detail of mathematical model of passive dampers like friction and MR damper. To understand the behavior of friction and MR damper, characterization of this dampers have been carried out through MATLAB under the sinusoidal and different earthquake excitations, namely El Centro, Kobe, Loma Prieta, and Northridge excitations, and Force Vs time, Force Vs Displacement, and Force Vs Velocity plots are obtained.

Chapter 4

Three Storey Shear Building Problem

4.1 General

The dynamic analysis of 3 - storey RC framed building through MATLAB is carried out in this chapter. The equation of motion for the building, 'uncontrolled building' i.e without passive devices are derived. Also, derivation of dynamic equation of motion for building with passive devices like friction and MR damper. Response quantities like displacement, velocity, acceleration, inter storey drift are determined under four different earthquake ground motion namely El-Centro, Kobe, Loma-Prieta and Northridge.

4.2 Building Data

- No. of Storey = G+2 Storey
- Story Height = 3 m
- Slab Thickness. = 120 mm
- No. of Bays in X-Direction = 3

- No. of Bays in Y-Direction = 3
- Bay Width in X-Direction = 4 m
- Bay Width in Y-Direction = 4 m
- Column Size = 0.3 m × 0.3 m
- Beam Size = 0.23 m × 0.3 m
- f_{ck}= 25 N/mm^2 (M 20 grade of concrete)
- f_y = 415 N/mm^2 (Fe 415 grade of steel)
- Live Load on Typical Storey = 3 KN/m^2

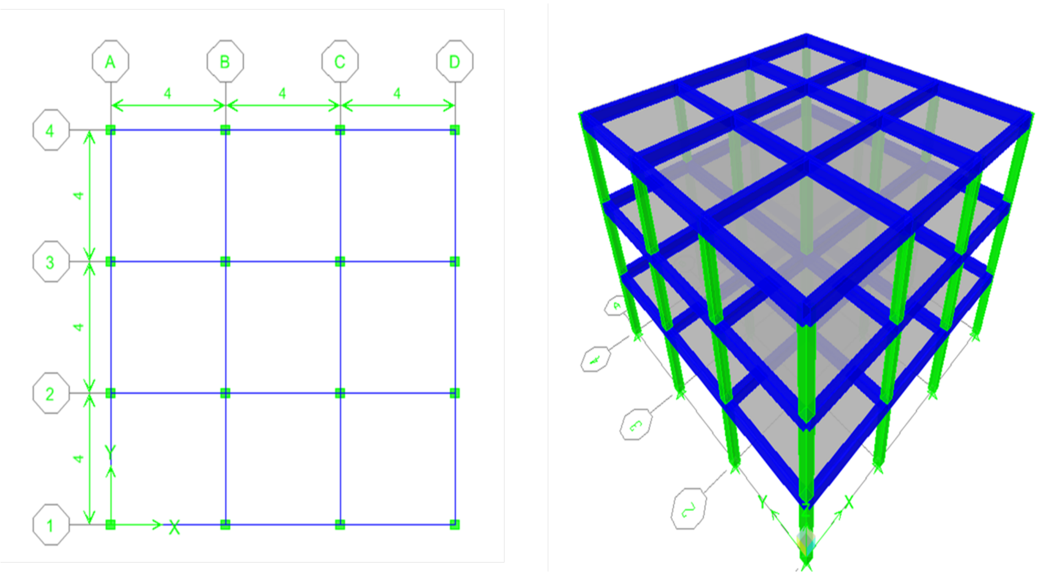

Figure 4.1: Three Storey Buildings Plan and 3D view

The building is symmetric in plan. Using lumped mass modeling approach is considered and Dynamic properties of the building like mass matrix and stiffness matrix is determined .Inherent damping of the building is assumed to be Rayleigh's damping (proportional damping), It is determined considering damping for first two mode is 5 % of critical damping. Detailed calculation of mass, stiffness and damping matrices are given in Appendix-A.

4.3 Equation of Motion for Uncontrolled Building

Consider a three storey reinforced concrete (RC) building as shown in Figure 4.1. For dynamic analysis lumped mass of the building is considered for dynamic analysis. The masses are assumed to be connected by mass-less elastic damping members. Linear or angular coordinates (degree of freedom) are used to describe the motion of the lumped masses, such model are called lumped masses or discrete mass model and is used in present study for analysis. Note that, 3-D building is a continuous system and this requires infinite numbers of degree of freedom to describe the motion of the building. However, here it is assumed that assumption slab is considered as rigid diaphragm help in deriving simplified model with limited degree of freedom . Figure 4.2 shows the simplified model of building with degree of freedom associated for present study.

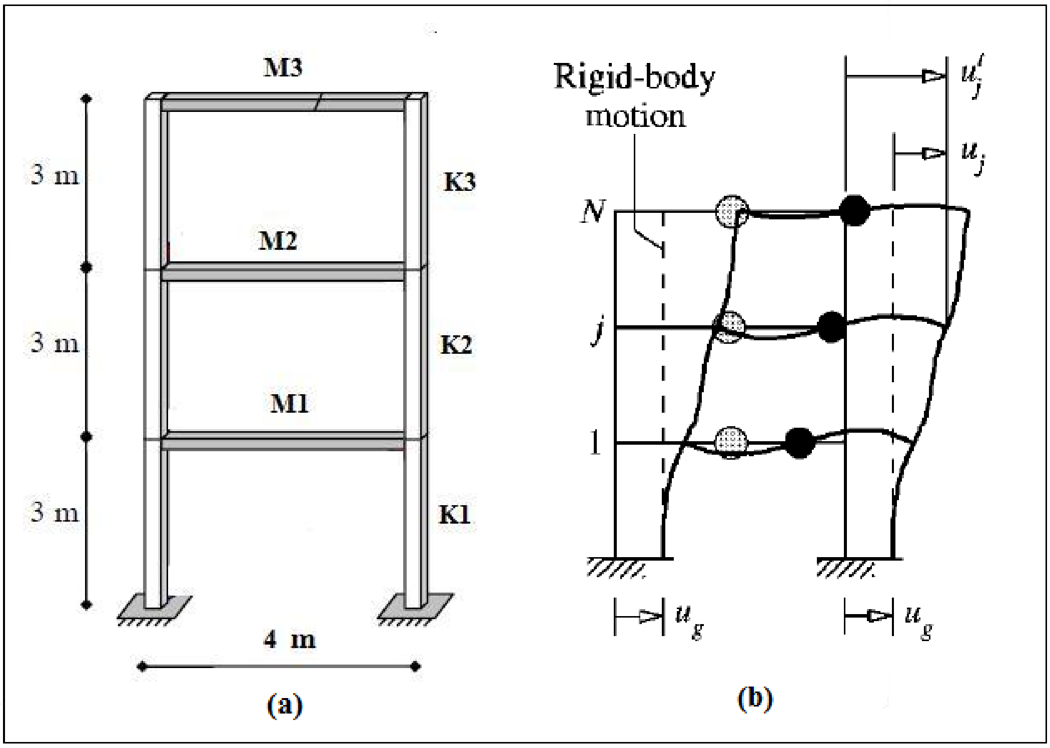

Figure 4.2: Three Storey Building: a) Lumped Mass Model, b)Building Frame under Ground Excitation

The equation of motion of uncontrolled building subjected to earthquake induced ground motion are derived first, to visualize elastic, damping, and inertia forces. In the building , the beam and floor system are considered rigid (infinitely stiff) in flexure, and several factors are neglected while deriving simplified model, like axial deformation of the beam and columns, and the effects of axial force on the stiffness of the columns. The mass is distributed uniformly throughout the building, but it is idealize as concentrated at the floor levels. The building as shown in Figure 4.2, has lump mass at each floor level and has three degree of freedoms: the lateral displacements u_1, u_2 and u_3 of the three floors in the direction of the x-axis.

According to D'Alembert's principle, with inertia forces included, a dynamic system is in equilibrium at each time instant. Each inertia force is equal to the product of mass times its acceleration and acts opposite to the direction of acceleration. The displacement of ground is denoted by u_g, the total or absolute displacement of mass by u^t; and the relative displacement between the mass and ground by u at each instant of time, these displacements are related by,

$$u^t(t) = u(t) + u_g(t) \tag{4.1}$$

Such equations for all the N masses can be combined in vector form:

$$u^t(t) = u(t) + u_g(t)l \tag{4.2}$$

Where the influence vector 'l' represents the displacement of the masses resulting from the static application of a unit ground displacement.

The equation of motion for the building of Figure 4.2 subjected to earthquake excitation can be derived by concept of dynamic equilibrium. The equation of dynamic equilibrium is,

$$f_I + f_D + f_S = 0 \tag{4.3}$$

Only the relative motion u between the mass and the base due to structural deformation produces elastic and damping forces. Thus for a linear system the damping force is,

$$f_D = c\dot{u} \tag{4.4}$$

And elastic resisting force is,

$$f_S = ku \tag{4.5}$$

The inertia force f_I is related to the total acceleration $\ddot{u}^t$ at the mass by,

$$f_I = m\ddot{u}^t \tag{4.6}$$

Substituting Equation 4.4, 4.5 and 4.6, in equation 4.3, and using equation 4.2.,

$$m\ddot{u}^t + c\dot{u} + k(u) = 0 \tag{4.7}$$

$$m\ddot{u}(t) + c\dot{u}(t) + ku(t) = -ml\ddot{u}_g(t) \tag{4.8}$$

Equation 5.6 is known as the equation of motion for the building subjected to earthquake excitation. Where $\ddot{u}_g(t)$ is the ground acceleration and m, c, and k are the mass, damping and stiffness matrix respectively. For building with n degree of freedom, the size of matrix $[m]$, $[c]$, and $[k]$ is $n \times n$.

4.4 Equation of Motion for Building with Passive Devices

The addition of dampers into a building not only increases the stiffness of the structure but also provides a significant amount of damping [23]. This added stiffness and damping helps in reducing the response of the building when subjected to earthquake excitation. For a shear building with added passive dampers subjected to earthquake excitation, the equation of motion of the system combining building and dampers can be written as,

$$m\ddot{u}(t) + c\dot{u}(t) + ku(t) = -ml\ddot{u}_g(t) - BF \tag{4.9}$$

where,

m, k, and c are the mass, stiffness and damping matrices of the building respectively.

u = The vector of the relative displacements of the floors of the building.

l = Influence vector.

$\ddot{u}_g$ = The earthquake acceleration excitation.

B = The matrix derived based on placement of passive devices in the building.

$F = [F_1,\ F_2,\ F_3\ .....\ F_n]^T$ is the vector of control forces produced by passive dampers, Here n is the number of floor of the building.

The control force F for linear friction dampers is given by Equation 3.2. The equations of motion of the multi-story structure with friction damper under the external excitation that is earthquake ground motion, then p_{eff} = -ml$\ddot{u}_g$(t), in which $\ddot{u}_g$(t) is the earthquake ground acceleration and 'l' is an identity matrix so Equation 4.11 can then be expressed as,

$$m\ddot{u}(t) + c\dot{u}(t) + ku(t) = -ml\ddot{u}_g(t) - B[Fcsgn\dot{u}(t)] \tag{4.10}$$

Equation 4.10 is the equation of motion for multi degree of structure with friction damper. Depending on the slip force p_y can be determined and is an important variable. In Equation 4.10, c represent the matrix due to structural inherent damping and B$c_d\dot{u}(t)$ represent the additional damping due to friction damper in the building.

Similarly for Magneto-Rheological (MR) damper, the control force F produces due to stiffness coefficient k_d and damping coefficient c_d are given in Equation 3.6. The equation of motion for the multi degree of freedom shear type building with MR damper can then be expressed as,

$$m\ddot{u}(t) + c\dot{u}(t) + ku(t) = -ml\ddot{u}_g(t) - B[c_0\dot{y}_d + k_1(x_d - x_0] \tag{4.11}$$

In this equation 4.11,The control force produces by MR damper is found out using equation.

4.5 Solution of Equation of Motion using Numerical Method

Analytical solution of equation of the motion for a multi degree of freedom system is usually not possible if the excitation-applied force or ground acceleration varies arbitrarily with time. Such problem can be solved by the numerical methods i.e. Newmark-Beta and Runge-Kutta etc. There are two basic approaches to numerically evaluate the dynamic response. The first approach is numerical interpolation of the excitation and the second is numerical integration of the equation of motion. Both approaches are applicable to linear systems but the second approach is related to non-linear systems.

Many numerical integration methods are available for the solution of equation of motion specified in previous section. All the numerical integration method have two basic characteristics. First, they do not satisfy differential equation at all time t, but only at discrete time intervals, say Δ(t) apart. secondly, within each time interval Δ(t), a specific type of variation of the displacement u, velocity $\dot{u}$,and acceleration $\ddot{u}$ is assumed. Thus, several numerical integration methods are available depending on the type of variation assumed for u, $\dot{u}$ and $\ddot{u}$ within each time interval Δt.

4.5.1 Time stepping Methods

Equation of motion in the case of base excitation due to earthquake is given as,

$$m\ddot{u}(t) + c\dot{u}(t) + ku(t) = -m\ddot{u}_g(t) \tag{4.12}$$

Now, subject to initial conditions u_0=*u(0)*; and $\dot{u}_0$=$\dot{u}(0)$ usually the system is assumed to have a linear damping, but other forms of damping such as nonlinear damping can be considered. The applied force at discrete time intervals and the time increment Δt_i = t_{i+1} - t_i is usually take to be constant, although this is not necessary. The response is determine at discrete time instants t_i, denoted as time i; the displacement, velocity, and acceleration at the i^{th} step are denoted by u_i, $\dot{u}_i$ and $\ddot{u}_i$ respectively. These values are assumed to satisfy Equation 4.12 at time $i:$ as,

$$m\ddot{u}_i + c\dot{u}_i + ku_i = p_i \tag{4.13}$$

Where ku_i is the resisting force at time i; for linearly elastic but would depend on the prior history of displacement and velocity at time i if the system were inelastic. In subsequent section numerical procedure is presented, which enable us to determine the response quantities u_{i+1}, $\dot{u}_{i+1}$ and $\ddot{u}_{i+1}$ at time (i+1) step that satisfy Equation 4.12 at time i+1:

$$m\ddot{u}_{i+1} + c\dot{u}_{i+1} + ku_{i+1} = p_{i+1} \tag{4.14}$$

If the numerical procedure is applied successively with i = 0, 1, 2, 3,....The time stepping procedure gives the desired response at all times with the known initial conditions u_0 and $\dot{u}_0$.

Types of Time Stepping Methods

Three types of time stepping procedures are as follows:

1) Method based on the interpolation of the excitation function.

2) Method based on finite difference expressions for the velocity and acceleration.

3) Method based on the assumed variation of acceleration.

In a direct integration method, the system of equation of motion is integrated successively by using step by step numerical method. No transformation of equation of motion is needed prior to integration and using difference formulas that involve one or more increments of time usually approximates time derivatives. Basically two principle approaches used in the direct integration method: Explicit and implicit schemes. In an explicit scheme, the response quantity are expressed in terms of previously determined value of displacement, velocity, and acceleration. In an implicit scheme the difference equations are combine with the equation of motion, and the displacements are calculated directly by the solving the equation.

4.5.2 Newmark Beta Method [18,19]

The well known Newmark direct integration method is quite often used to compute the structural response, and hence in this section we intend to formulate a procedure that incorporates the Newmark type numerical scheme in solving the equation of motion with and without passive devices under the earthquake excitations.

The Newmark Beta integration method is based on the assumption that the acceleration varies linearly between two instants of time. Two parameter α and β are used in this method, which can be suit the requirement of the particular problem. Newmark [15] presented a family of time-step methods for the solution of structural dynamics problem for both blast and seismic loading. In order to illustrate the use of this numerical integration method, consider the solution of linear dynamic equilibrium equations of motion as given in Equation 4.14. Newmark developed a family of time-stepping methods based on the following equations:

$$\dot{u}_{i+1} = \dot{u}_i + [(1-\gamma)\Delta t]\ddot{u}_i + (\gamma \Delta t)\ddot{u}_{i+1} \tag{4.15}$$

$$u_{i+1} = u_i + (\Delta t)\dot{u}_i + [(0.5 - \beta)(\Delta t)^2]\ddot{u}_i + [\beta(\Delta t)^2]\ddot{u}_{i+1} \tag{4.16}$$

Newmark used Equations 4.14, 4.15 and 4.16 iteratively for each time step, for each displacement DOF of the structural system. The parameter β and γ define the variation of acceleration over a time step and determine the stability and accuracy characteristics of the method. Typical selection for γ is 1/2 and $1/6 \leq \beta \leq 1/4$ is satisfactory from all point of view, including that of accuracy. These two equations, combined with the equilibrium Equation 4.14 at the end of the time step, provide the basis for computing u_{i+1}, $\dot{u}_{i+1}$ and $\ddot{u}_{i+1}$ at time (i+1) from the known u_i, $\dot{u}_i$ and $\ddot{u}_i$ at time i. Iteration is required to implement these computations because the unknown $\ddot{u}_{i+1}$ appears in the right side of Equation 4.15 and 4.16. The parameter γ and β indicate how much acceleration enters into the displacement and velocity equations at the end of the interval Δt. Therefore, γ and β are chosen to obtain the desired integration accuracy and stability. When $\gamma = 1/2$ and $\beta = 1/6$, Equations 4.15 and 4.16 correspond to the linear acceleration method. When $\gamma = 1/2$ and $\beta = 1/4$, this correspond to the assumption that the acceleration remain constant. The complete algorithm using the Newmark Beta integration method is given in Table 4.1.

Table 4.1 Newmark's Direct Integration Method[6]

---

1) Initial calculation

(1.1) Form static stiffness matrix [k], mass matrix [m] and damping matrix [c]

(1.2) Specify integration parameter γ and β

(1.3) Select Δt

(1.4) Specify initial conditions u_0, $\dot{u}_0$, $\ddot{u}_0$

(1.5) $\ddot{u}_0 = \frac{p_0 - c\dot{u}_0 - ku_0}{m}$

(1.6) Calculate constants, a = $\frac{1}{\beta \Delta t}$m + $\frac{\gamma}{\beta}$c; and b = $\frac{1}{2\beta}$m + Δt($\frac{\gamma}{2\beta}$-1)c.

(1.7) Calculate modified stiffness, $\widehat{k}$ = k + $\frac{\gamma}{\beta \Delta t}$c + $\frac{1}{\beta(\Delta t)^2}$m.

2) Calculation for each time step, i

(2.1) $\Delta \widehat{p_i} = \Delta p_i$ + a$\dot{u}_i$ + b$\ddot{u}_i$

(2.2) $\Delta u_i = \frac{\Delta \widehat{p}_i}{\widehat{k}}$

(2.3) Δ $\dot{u}_i = \frac{\gamma}{\beta \Delta t}\Delta u_i$ - $\frac{\gamma}{\beta}$ $\dot{u}_i$ + Δt(1-$\frac{\gamma}{2\beta}$)$\ddot{u}_i$.

(2.4) Δ $\ddot{u}_i = \frac{1}{\beta(\Delta t)^2}\Delta u_i$ - $\frac{1}{\beta \Delta t}$ $\dot{u}_i$ - $\frac{1}{2\beta}\ddot{u}_i$

(2.5) $u_{i+1} = u_i + \Delta u_i$, $\dot{u}_{i+1} = \dot{u}_i + \Delta \dot{u}_i$ and $\ddot{u}_{i+1} = \ddot{u}_i + \Delta \ddot{u}_i$

3) Repetition for the next time step. Replace i by $i + 1$ and implement steps 2.1 to 2.5 for the next time step.

For the ground acceleration excitation $\ddot{u}_g$(t), replace p_i by -m$\ddot{u}_{gi}$ in Table 4.1. The computed u_i, $\dot{u}_i$, and $\ddot{u}_i$ gives response value like displacement, velocity and acceleration relative to the ground. We can find out the total velocity and total acceleration from $\dot{u}_i^t = \dot{u}_i + \dot{u}_{gi}$ and $\ddot{u}_i^t = \ddot{u}_i + \ddot{u}_{gi}$, respectively.

4.6 Response of Uncontrolled Shear Building

In this section, response of uncontrolled shear building is obtained under four different types of earthquakes excitations. Earthquake excitation considered are, El Centro, Loma Prieta, Kobe, and Northridge, where first two excitation are strong motion type while later two excitation are pulse type motion. In order to obtain response quantity equation of motion given by Equation 5.6 is solved using Runge-Kutta method discussed in Section 4.5 through writing code in MATLAB. Response quantities like displacement, acceleration, inter storey drift and velocity are extracted for a shear building.

4.7 Result and Discussions

Table 4.1 shows the maximum response quantity obtained for uncontrolled building under El Centro earthquake excitation.

Table 4.1: Response Quantity under El Centro (PGA-0.3129g) EQ

Storey	**Max.Displ** (m)	**Max.Velo** (m/sec)	**Max. Accel** (m/sec^2)	**Inter Storey Drift** (m)
1	0.010	0.197	5.476	0.011
2	0.018	0.327	7.107	0.008
3	0.023	0.386	8.382	0.005

It is evident that maximum displacement, maximum velocity, and maximum acceleration increases with storey numbers. i,e,. maximum response occurs at top storey of the building. However, inter storey drift is maximum at lower storey and decreases with storey numbers. Time history plot of response quantities like, displacement, acceleration and velocity is obtained. Figure 4.3 shows time history plot of displacement, velocity and acceleration for top storey of the building. It is seen that maximum displacement is 23 mm, maximum velocity is 38.6 cm/sec and maximum acceleration is 838 cm/s^2. It is also observed that, response quantities shows increased response when frequency of earthquake excitation increases.

Similarly, response quantity like displacement, velocity, and acceleration are also obtained for uncontrolled building under Kobe, Loma Prieta, and Northridge earthquake excitations. Table 4.2 to 4.4 shows that maximum displacement, maximum velocity, and maximum acceleration increases with storey numbers, however inter storey drift is maximum at lowest storey and decreases with storey numbers.

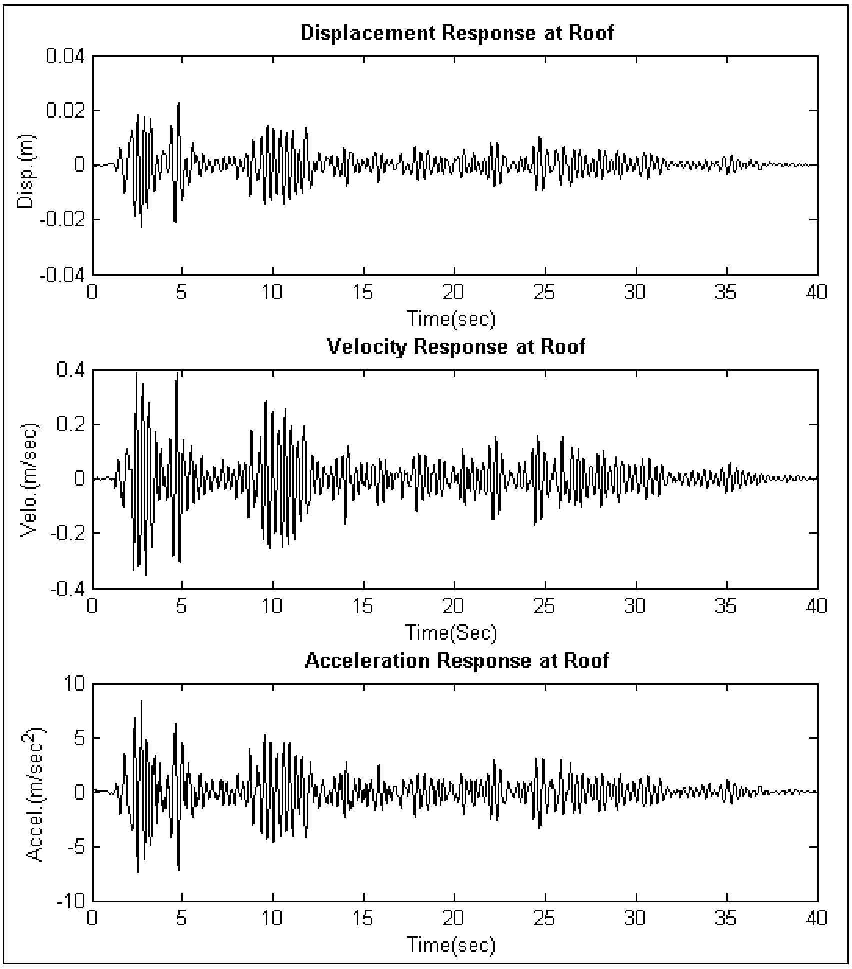

Figure 4.3: Uncontrolled Building Response at Roof under El Centro EQ Excitation

Figure 4.4 to 4.6 shows the time history of building at roof under the Kobe, Loma Prieta, and Northridge, respectively. From Figure 4.4, it is seen that maximum displacement is 55 mm, maximum velocity is 79.2 cm/sec and maximum acceleration is 1782.3 cm/s^2. It is also observed that, response quantity shows increased response when frequency of earthquake excitation increases. Time history under the Loma Prieta earthquake are shown in Figure 4.5, it is seen that maximum displacement is 62 mm, maximum velocity is 125 cm/sec and maximum acceleration is 2111.9 cm/s^2.

Table 4.2: Response Quantity under Kobe (PGA-0.6936g) EQ

Storey	**Max.Displ** (m)	**Max.Velo** (m/sec)	**Max. Accel** (m/sec^2)	**Inter Storey Drift** (m)
1	0.026	0.422	9.673	0.031
2	0.045	0.692	14.623	0.024
3	0.055	0.792	17.823	0.012

Table 4.3: Response Quantity under Lomaprieta (PGA-0.6437g) EQ

Storey	**Max.Displ** (m)	**Max.Velo** (m/sec)	**Max. Accel** (m/sec^2)	**Inter Storey Drift** (m)
1	0.029	0.553	10.279	0.029
2	0.051	1.007	16.791	0.023
3	0.062	1.251	21.119	0.012

Table 4.4: Response Quantity under Northridge (PGA-1.585g) EQ

Storey	**Max.Displ** (m)	**Max.Velo** (m/sec)	**Max. Accel** (m/sec^2)	**Inter Storey Drift** (m)
1	0.044	0.770	16.318	0.044
2	0.078	1.508	25.418	0.034
3	0.095	1.904	31.330	0.017

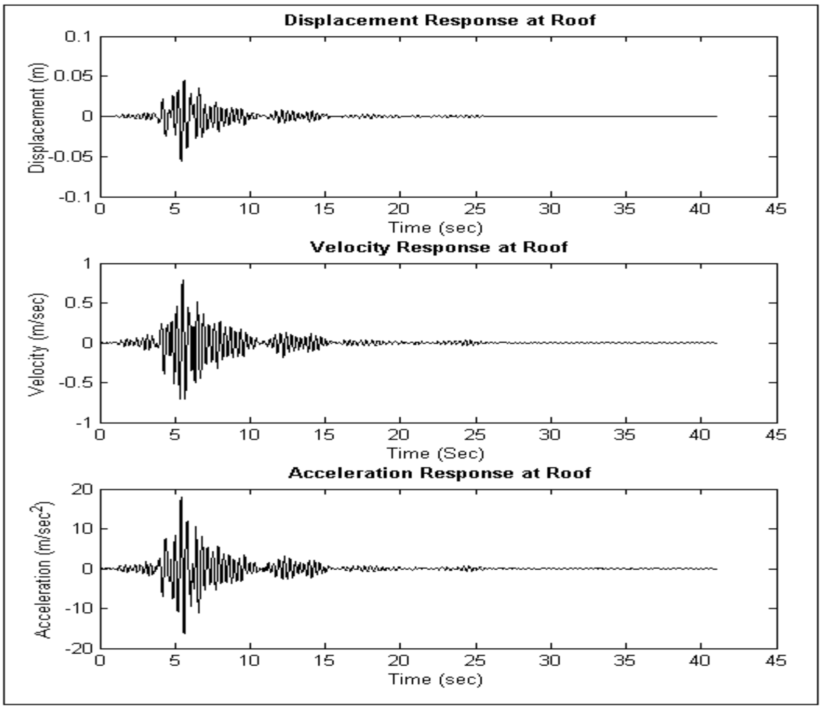

Figure 4.4: Uncontrolled building Response at Roof under Kobe EQ Excitation

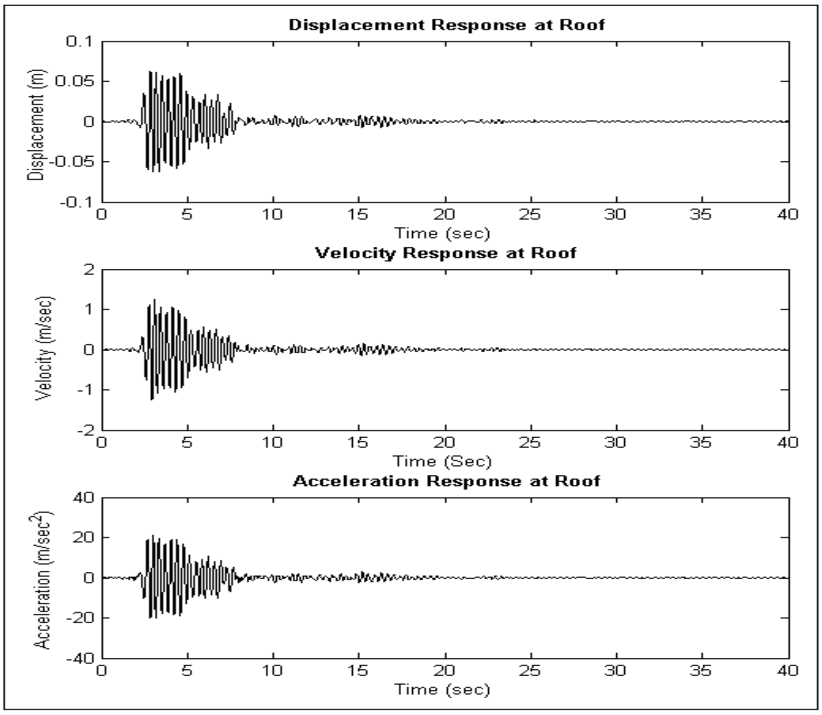

Figure 4.5: Uncontrolled building Response at Roof under Loma Prieta EQ Excitation

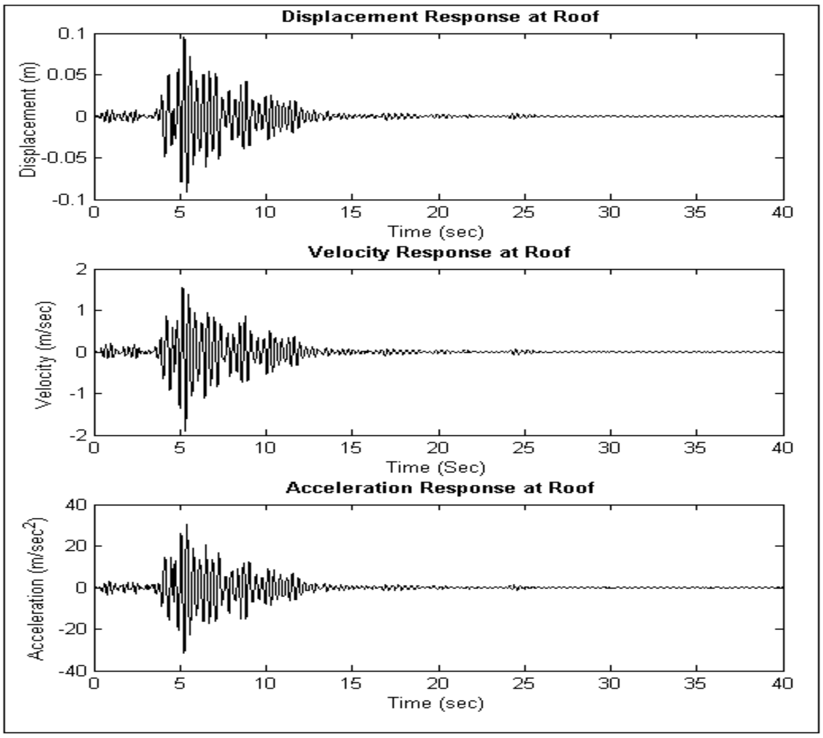

Figure 4.6: Uncontrolled building Response at Roof under Northridge EQ Excitation

Figure 4.6 shows time history plot of displacement, velocity and acceleration for top storey of the building. It is seen that maximum displacement is 95 mm, maximum velocity is 190.4 cm/sec and maximum acceleration is 3133.0 cm/s^2. It is also observed that, response quantities shows increased response when frequency of earthquake excitation increases.

4.8 Summary

The chapter deals with the dynamic response of uncontrolled shear building. Equation of motion for uncontrolled and controlled building with passive devices like friction and MR damper are derived. Using Newmark-Beta method response quantiies of building are find out like maximum displacement, maximum velocity, maximum acleration and inter storey drift under the four different earthquake excitations.

Chapter 5

Response of Building using Friction Damper

The chapter deals with the response of shear building using friction damper. The time history direct integration method Newmark-Beta is used to find out the response quantity of controlled structure. Algorithm of Newmark-Beta method given in Table 4.1, is used to find out the different response quantities through MATLAB. Extraction of different response quantities are given in subsequent sections.

Primarily using automotive brakes as an analogy Pall et al. (1980) began the development of friction devices to improve the seismic response of the structures. In the inverting years, number of friction devices have been developed, such as the X-braced friction devices illustrated in figure (Pall and Marsh 1982), the Sumitomo friction damper, and slotted bolted connection. The devices differ in their mechanical complexity and in the materials used for the sliding surfaces. Generally, friction devices generate rectangular hysteretic loops similar to the characteristic of Coulomb friction. After a hysteric restoring force model has been validated for a particular device, the device model can be rapidly incorporated into an overall structural analysis.

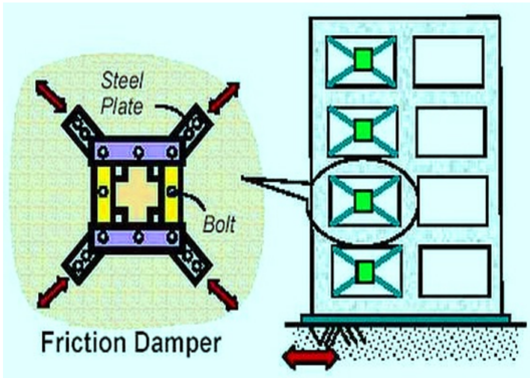

Figure 5.1: A structure with passive damper

5.1 Design of Friction Damper

The concept of replacing the complicated and often nonlinear behavior of damper by equivalent linear stiffness and viscous characteristic has enormous benefits for the preliminary analysis and design of the damper added structure. These devices dissipate energy through yielding of metallic or through sliding contact friction between adjoining surfaces. They can be considered hysteretic devices since their energy dissipation depends primarily on relative displacement within the device, and their energy dissipation is not sensitive to the velocity. Thus they can be modeled with force-displacement hysteretic relationship.

Some typical models that have been used to represent the nonlinear force-displacement relationship are the simple elastoplastic model, the bilinear model, and the polynomial model [4]. The cyclic hysteretic characteristic of these models is based on their skeleton curve, which is the name given their monotonic force-displacement curve. The area contained within one cycle of the hysteretic curve is the energy dissipated per cycle. The equivalent viscous damping is obtained by setting the area within the hysteretic loop equal to the area within a viscous damper cycle.

Elastoplastic Form: The initial elastic stiffness is determined from experimental yield force and yield displacement data as

$$k_e = p_y/d_y \tag{5.1}$$

Whenever the device displacement exceeds d_y the force is equal to py. The energy dissipated per cycle(E) is equal to the area within the hysteretic loop between (p_y,d_0) and ($-p_y$,$-d_0$) which is

$$E = 4p_y(d_0 - d_y), d_0 >= d_y \tag{5.2}$$

Figure shows typical cyclic hysteretic shapes of a friction devices; these shapes are

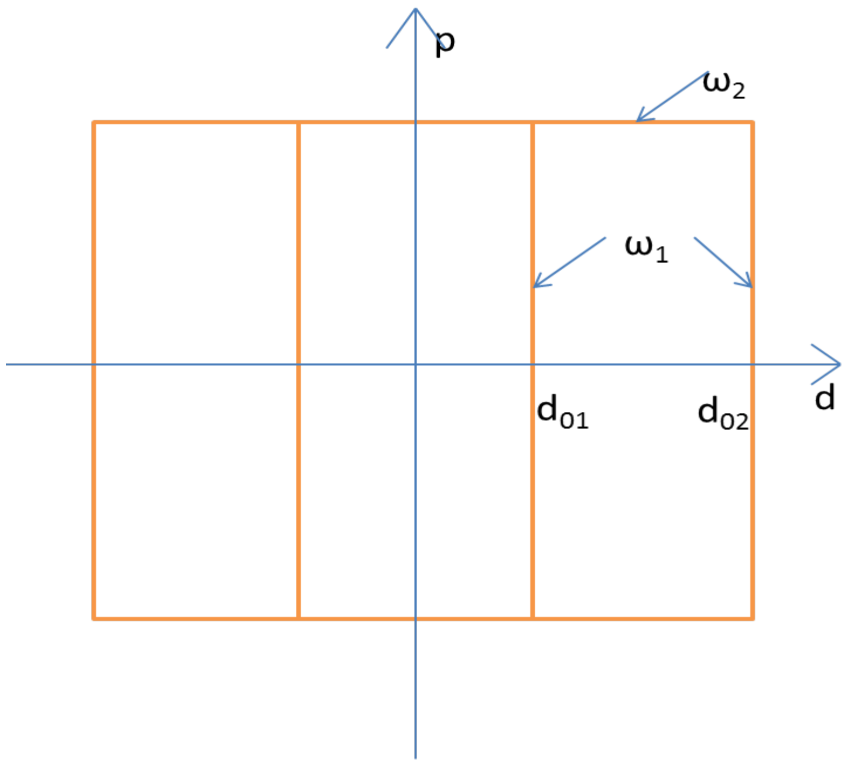

Figure 5.2: Friction device damper

based on the mechanical properties of the devices and on experimental data. For a friction damper, the elastoplastic model with $d_y = 0$ os quite adequate.Figure also indicate that for friction damper, the hysteretic loops at same maximum device displacement remain essentially unchanged at various excitation frequencies, thus demonstrating their rate-independent property This equation of motion is solved using numerical method Newmark-Beta as per Table 4.1 for four different types of earthquake excitations through MATLAB. The response quantities like relative displacement, relative velocity, absolute acceleration and damper forces for different value of damping co-efficient 'C_d' are calculated. The earthquake excitations used in this study are given in Table 3.2.

5.1.1 Equivalent Viscous Damping and Stiffness

Consider a simple one storey elastic structure with velocity-proportional viscous damping. The equation of motion is

$$m\ddot{x} + c\dot{x} + kx = -m\ddot{x}_g \tag{5.3}$$

where $\ddot{x}$,$\dot{x}$ and x are the horizontal structure acceleration, velocity and displacement

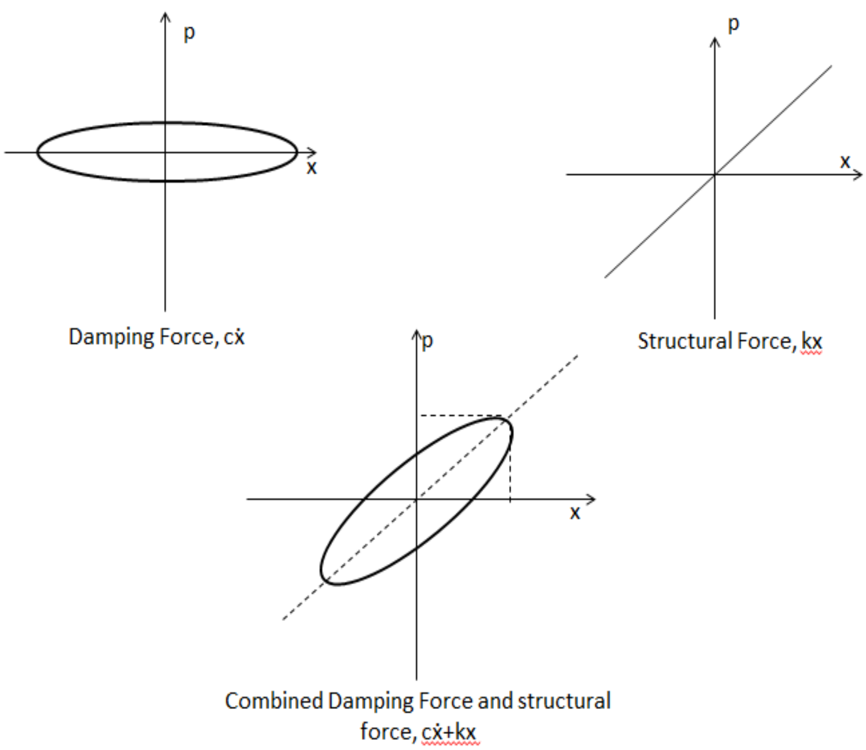

Figure 5.3: Damping and structural restoring forces

relative to the foundation; $\ddot{x}_g$ is the horizontal acceleration of the foundation caused by earthquake; and m, c and k are mass, viscous damping and stiffness of the structure. The c$\dot{x}$ and kx terms are illustrated in figure . The structure reactive force can be defined as c$\dot{x}$+kx. Note that maximum force,p_{max}, does not occur at the same time as the maximum displacement,x_{max}. The energy dissipated per cycle is equal to the area of the ellipse described by

$$E = (2\pi^2 c x_0^2)/T \tag{5.4}$$

Where x_0 is the maximum amplitude of the cyclic displacement, and T is the period of the cyclic motion. For elastoplastic model, setting E equal to viscous E-value results in an equivalent viscous damping coefficient of

$$c_d = 4p_y(d_0 - d_y)/(2\pi^2 d_0^2) \tag{5.5}$$

Where d_0 is the maximum device displacement corresponding to maximum structural displacements, x_0. It can be seen that the equivalent viscous damping is inversely related to the maximum cyclic displacement, d_0, and proportional to the cyclic response period,T.

For a friction device, p_y becomes the slip force, and $d_y \longrightarrow 0$ and $k_e \longrightarrow \infty$ such that $d_y\ k_e = p_y$. Thus, the equivalent viscous damping is proportional to the device slip force and the cyclic period of response,T and is inversely proportional to the maximum cyclic displacement, d_0. In this case, $k_d = 0$ when sliding occurs.

5.1.2 Calculation of Equivalent Viscous Damping

- The design is carried out according to R. D. Hanson and T. T. Soong [4], which recommends Equivalent viscous damping for analysis.

- The procedure for design was given in above section. Calculation usually comprise of estimating additional stiffness and damping provided by the damper which were calculated by Equations 5.1, 5.4 and 5.5.

- Slip force is generally 15 to 30% of total weight of the building.
- Total Weight of the building = 2278.80 kN.For finding the damping value C_d, therefore slip force is 684.64 kN (considering 30 % of total weight of the building)
- Device displacement =24.47 mm (85 % of the structural design limit)
- Time period = 0.351 sec (As per dynamic analysis of the building)

Data Taken:

Total weight of the building, ω	69688.07 kg
Inherent Damping Ratio of Building	5%
Storey Drift Ratio	0.40%
Operating Temperature, T	25^oC
Storey Height, h	3 m
Required Damping Ratio, ζ	20%
Angel Between Bracing Member and Floor, θ	36.86
Time Period, (T)	15%

1) In this study of Friction damper design, Maximum design damper deformation is $0.004 \times 0.012 \times h \times cos\theta = 0.0244$ m.

2) Attachment coefficient for calculating damping coefficient given in table -7 [23]

$$\cos^2 \theta$$

$$\alpha_d = (\cos(37.89))^2 = 0.622$$

3) Slip load for friction damper is generally 15 to 30 % of total weight of the building.

$$\text{So slip force} = 0.30\times \text{ total weight of the building} = 0.30\times\ 2278800.02 \text{ kN} = 683.64 \text{ kN}$$

4) Determining damping coefficient

$$c_d = 4p_y(d_0 - d_y)/(2\pi^2 d_0^2) \tag{5.6}$$

So from $c_d = 1244$ kN sec m

5.2 Results and Discussion

This section presents the results obtained through direct integration method Newmark-Beta of three storey R.C. frame building with displacement dependent energy dissipation device i.e friction damper. The response of R.C frame building in the form of relative displacement, relative velocity, absolute acceleration, and damper force are obtained. Efficiency of these damping systems is investigated for four earthquake excitation of different peak acceleration value, namely El Centro, Kobe, Loma Prieta and Northridge. The undamped structural response was found out as discussed in Section 4.6 of chapter 4 in order to compare its results with the results of the building embedded with friction damping system. There are various ways of assessing seismic response, but computation of top storey response is a reasonable measure of the overall effect of seismic response. The reduction in the top storey velocity, acceleration, and damping force at first storey of the building are also investigated for four types of earthquake excitations.

5.2.1 Comparison of Displacement Response

The results of displacement response of uncontrolled and controlled building for four earthquake excitation of different peak acceleration value, namely El Centro, Kobe, Loma Prieta and Northridge are given in Table 5.1 to 5.4 respectively. The graphical representations of comparison of displacement response for uncontrolled and controlled structure are presented in Figure 6.1. From results, it is evident that displacement of top storey is highest, so comparison of displacement is done at top of the building.

Table 5.1: Relative Displacement under El Centro (PGA-0.3129g) EQ Excitation

Maximum Storey Displacement (m)						
	1^{st}	% Red.	2^{nd}	% Red.	Roof	% Red.
Controlled	0.0079	24.76	0.0144	20	0.023	22.6
Uncontrolled	0.010	0.0	0.0184	0.0	0.0228	0.0

Table 5.2: Relative Displacement under Kobe (PGA-0.6936g) EQ Excitation

Maximum Storey Displacement (m)						
	1^{st}	% Red.	2^{nd}	% Red.	Roof	% Red.
Controlled	0.0179	31.15	0.0330	26.66	0.0410	25.45
Uncontrolled	0.026	0.0	0.045	0.0	0.055	0.0

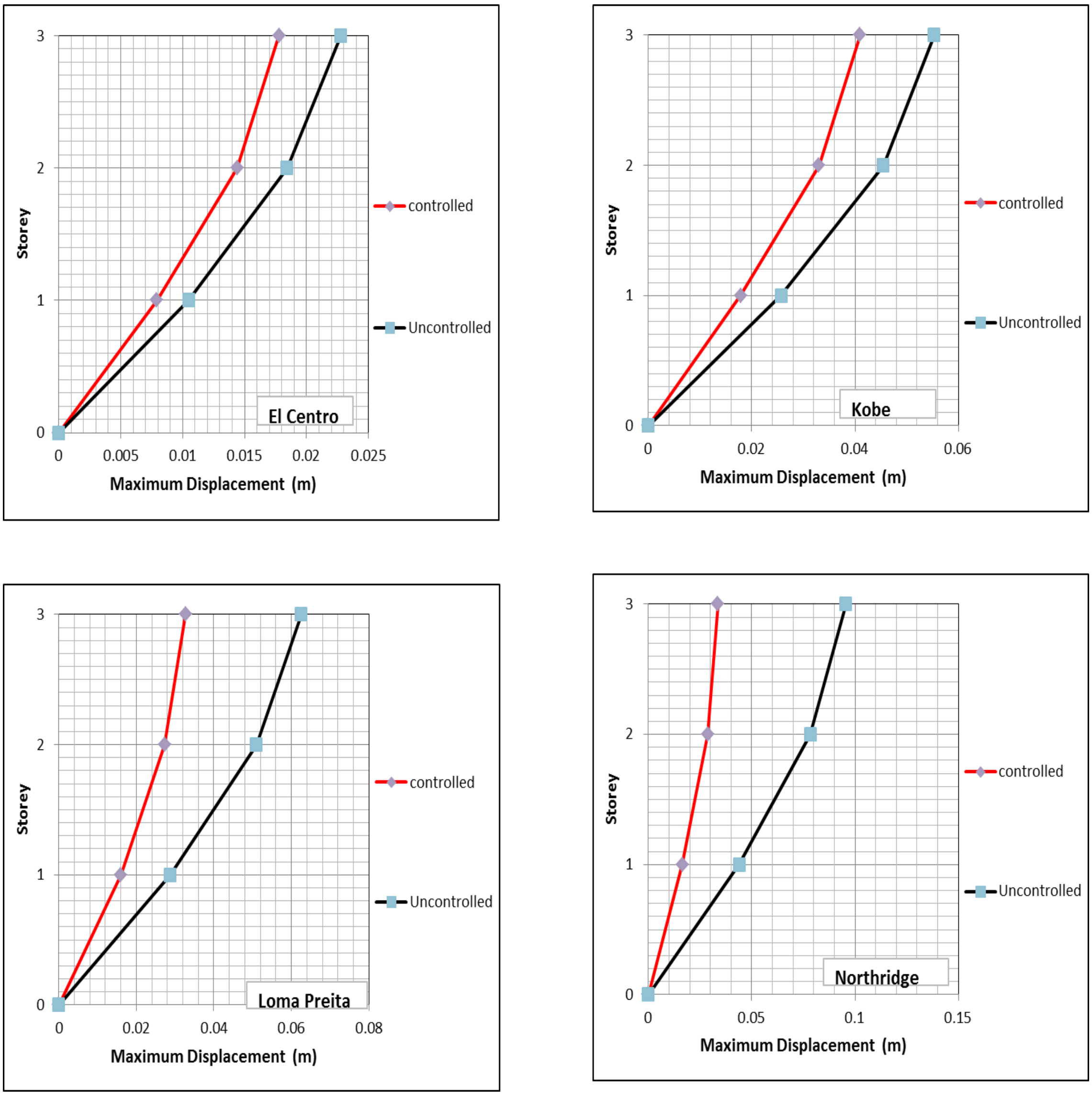

Figure 5.4: Comparison of Displacement for Different EQ Excitation

Table 5.3: Relative Displacement under Lomaprieta (PGA-0.6437g) EQ Excitation

Maximum Storey Displacement (m)						
	1^{st}	% Red.	2^{nd}	% Red.	Roof	% Red.
Controlled	0.0160	44.25	0.0273	46.36	0.0327	47.68
Uncontrolled	0.0287	0.0	0.0509	0.0	0.0625	0.0

Table 5.4: Relative Displacement under Northridge (PGA-1.585g) EQ Excitation

Maximum Storey Displacement (m)						
	1^{st}	% Red.	2^{nd}	% Red.	Roof	% Red.
Controlled	0.0165	62.41	0.0287	63.34	0.0337	64.67
Uncontrolled	0.0439	0.0	0.0783	0.0	0.0954	0.0

For controlled building with friction damper a reduction of 22.60%, 25.45%, 47.68% and 64.67% in roof displacement is observed, when co-efficient of damping 'C_d' is 1244 $kN \cdot sec/cm$ for El Centro, Kobe, Loma Prieta and Northridge earthquake excitations, respectively, with respect to uncontrolled structure. But for Northridge earthquake 64.67% roof displacement reduction is observed, which is very high as compare to other three earthquake excitations for C_d=1244 $kN \cdot sec/cm$. It is observed that, reduction in displacement up to 47% is achieved when friction damper with co-efficient of damping C_d=1244 $kN \cdot sec/cm$ is used, under Loma Prieta earthquake excitations.

5.2.2 Comparison of Velocity Response

The results of Velocity response of uncontrolled and controlled building for four earthquake excitation of different peak acceleration value, namely El Centro, Kobe, Loma Prieta and Northridge are given in Table 6.5 to 6.8, respectively. The graphical representations of comparison of velocity for uncontrolled and controlled structure are presented in Figure 6.2.

Table 5.5: Relative Velocity under El Centro (PGA-0.3129g) EQ Excitation

Maximum Storey Velocity (m/sec)						
	1^{st}	% Red.	2^{nd}	% Red.	Roof	% Red.
Controlled	0.1611	18.22	0.256	21.71	0.336	5
Uncontrolled	0.197	0.0	0.327	0.0	0.386	0.0

Table 5.6: Relative Velocity under Kobe (PGA-0.6936g) EQ Excitation

Maximum Storey Velocity (m/sec)						
	1^{st}	% Red.	2^{nd}	% Red.	Roof	% Red.
Controlled	0.378	10.42	0.636	8	0.737	7
Uncontrolled	0.422	0.0	0.692	0.0	0.792	0.0

Table 5.7: Relative Velocity under Lomaprieta (PGA-0.6437g) EQ Excitation

Maximum Storey Velocity (m/sec)						
	1^{st}	% Red.	2^{nd}	% Red.	Roof	% Red.
Controlled	0.198	64.19	0.348	65.9	0.427	66.03
Uncontrolled	0.553	0.0	1.007	0.0	1.257	0.0

Table 5.8: Relative Velocity under Northridge (PGA-1.585g) EQ Excitation

Maximum Storey Velocity (m/sec)						
	1^{st}	% Red.	2^{nd}	% Red.	Roof	% Red.
Controlled	0.244	69.31	0.474	68.56	0.587	69.17
Uncontrolled	0.770	0.0	1.508	0.0	1.904	0.0

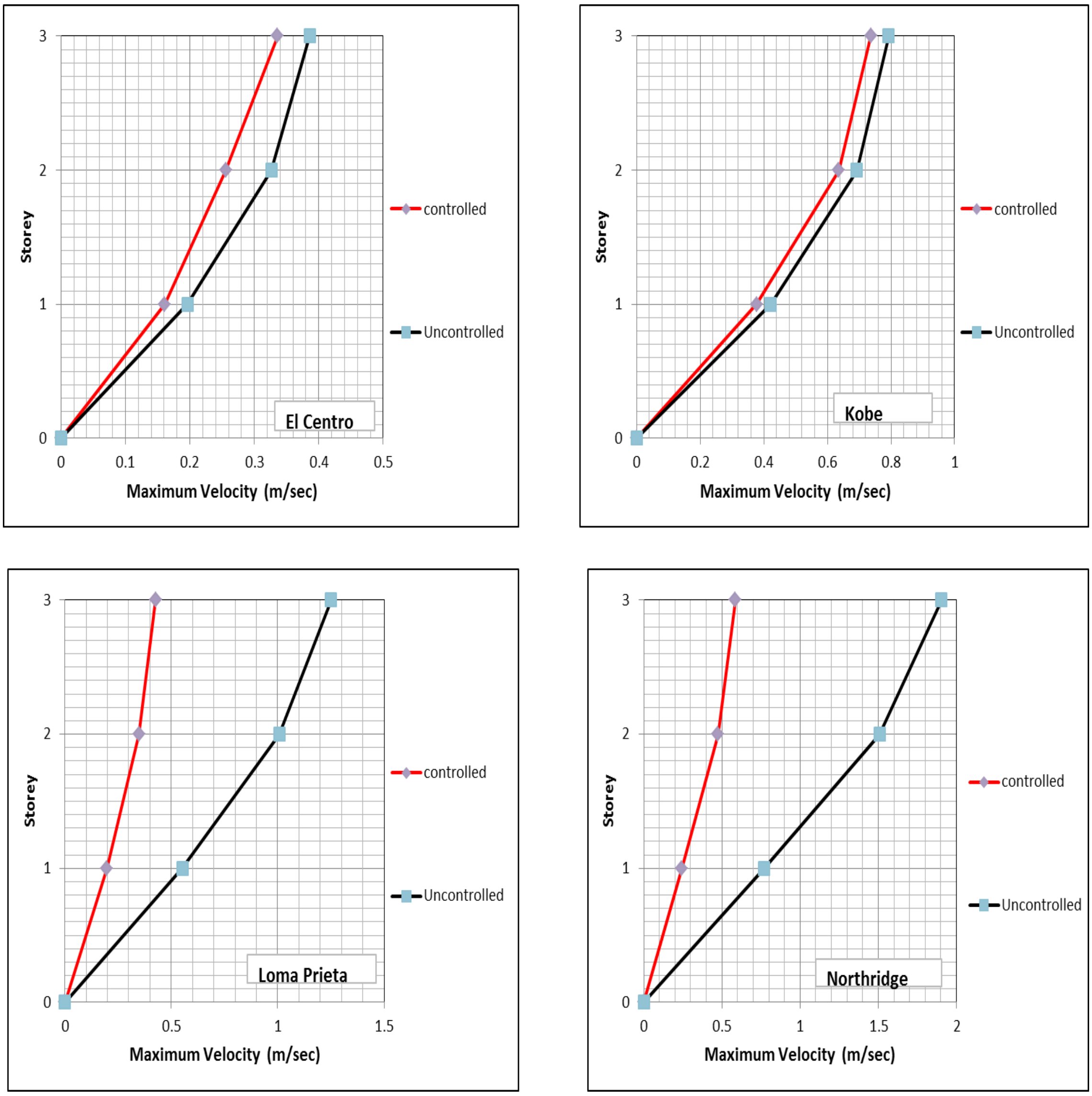

Figure 5.5: Comparison of Velocity for Different EQ Excitation

From results, it is evident that velocity of top storey is highest, so comparison of velocity is done at top of the structure. For controlled building with friction damper a reduction of 5%, 7%, 66.03% and 69.17% in roof velocity is observed, when co-efficient of damping 'C_d' is 1244 $kN \cdot sec/cm$ for El Centro, Kobe, Loma Prieta and Northridge earthquake excitation, respectively, with respect to uncontrolled structure. But for Northridge and Loma Prieta earthquake 66.78% and 66.03% roof velocity reduction is observed respectively, which is very much higher as compare to other two earthquake excitations.

5.2.3 Comparison of Acceleration Response

The results of acceleration response of uncontrolled and controlled building for four earthquake excitation of different peak acceleration value, namely El Centro, Kobe, Loma Prieta and Northridge are given in Table 6.9 to 6.12 respectively. The graphical representations of comparison of acceleration response for uncontrolled and controlled structure are presented in Figure 6.3.

Table 5.9: Absolute Acceleration under El Centro (PGA-0.3129g) EQ Excitation

Maximum Storey Acceleration (m/sec^2)						
	1^{st}	% Red.	2^{nd}	% Red.	Roof	% Red.
Controlled	2.90	47.04	5.10	28.23	6.23	25.67
Uncontrolled	5.476	0.0	7.107	0.0	8.382	0.0

Table 5.10: Absolute Acceleration under Kobe (PGA-0.6936g) EQ Excitation

Maximum Storey Acceleration (m/sec^2)						
	1^{st}	% Red.	2^{nd}	% Red.	Roof	% Red.
Controlled	4.856	49.79	10.080	31.06	13.126	26.35
Uncontrolled	9.673	0.0	14.623	0.0	17.823	0.0

Table 5.11: Absolute Acceleration under Loma Prieta (PGA-0.6437g) EQ Excitation

Maximum Storey Acceleration (m/sec^2)						
	1^{st}	% Red.	2^{nd}	% Red.	Roof	% Red.
Controlled	2.924	71.44	5.550	66.94	7.014	66.78
Uncontrolled	10.279	0.0	16.791	0.0	21.119	0.0

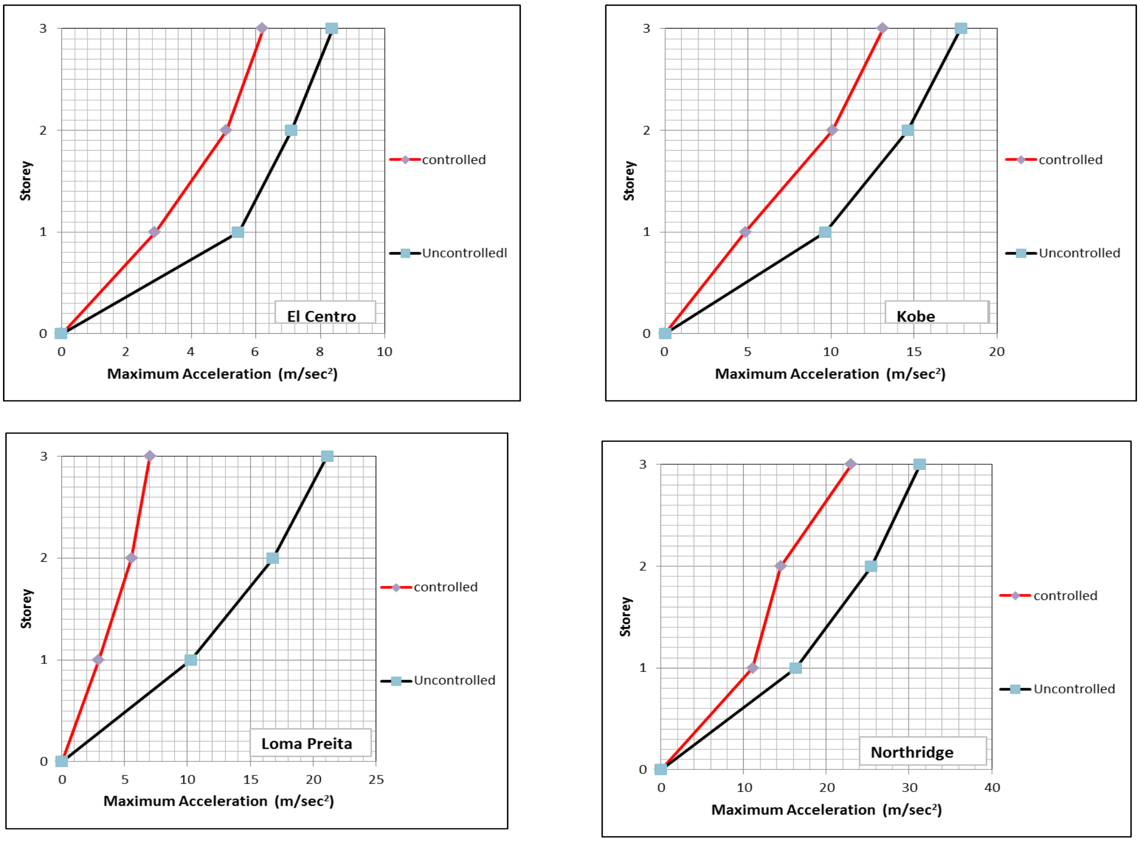

Figure 5.6: Comparison of Acceleration for Different EQ Excitation

Table 5.12: Absolute Acceleration under Northridge (PGA-1.585g) EQ Excitation

Maximum Storey Acceleration (m/sec^2)						
	1^{st}	% Red.	2^{nd}	% Red.	Roof	% Red.
Controlled	11.115	31.88	14.477	43.04	23.230	25.53
Uncontrolled	16.318	0.0	25.418	0.0	31.330	0.0

From results, it is evident that acceleration of top storey is highest, so comparison of acceleration is done at top of the structure. For controlled building with friction damper reduction is 25.67%, 26.67%, 66.78% and 25.53% in roof acceleration is observed, when co-efficient of damping 'C_d' is 1241 $kN \cdot sec/cm$ for El Centro, Kobe, Loma Prieta and Northridge earthquake excitation, respectively, with respect to uncontrolled structure. But for El Centro and Kobe earthquake reduction is 66.78% in roof acceleration is observed, which is higher as compare to other three earthquake excitations.It is observed that, reduction in roof acceleration up to 25% is achieved when damper with co-efficient of damping 'C_d'=1244 $kN \cdot sec/cm$ is used, under Loma Prieta, Northridge and Kobe type of earthquake excitations.

5.2.4 Comparison of Inter Storey Drift

The results of inter storey drift of uncontrolled and controlled building for four earthquake excitation of different peak acceleration value, namely El Centro, Kobe, Loma Prieta and Northridge are given in Table 6.13 to 6.16 respectively. The graphical representations of comparison of inter storey drift for uncontrolled and controlled structure are presented in Figure 6.4.

Table 5.13: Inter Storey Drift under El Centro (PGA-0.3129g) EQ Excitation

Maximum Inter Storey Drift (m)						
	1^{st}	% Red.	2^{nd}	% Red.	Roof	% Red.
Controlled	0.007	44.82	0.006	52.17	0.003	58.33
Uncontrolled	0.011	0.0	0.008	0.0	0.005	0.0

Table 5.14: Inter Storey Drift under Kobe (PGA-0.6936g) EQ Excitation

Maximum Inter Storey Drift (m)						
	1^{st}	% Red.	2^{nd}	% Red.	Roof	% Red.
Controlled	0.017	45.16	0.0015	37.5	0.003	75
Uncontrolled	0.031	0.0	0.024	0.0	0.012	0.0

Table 5.15: Inter Storey Drift under Lomaprieta (PGA-0.6437g) EQ Excitation

Maximum Inter Storey Drift (m)						
	1^{st}	% Red.	2^{nd}	% Red.	Roof	% Red.
Controlled	0.016	44.82	0.011	52.17	0.005	58.33
Uncontrolled	0.029	0.0	0.023	0.0	0.012	0.0

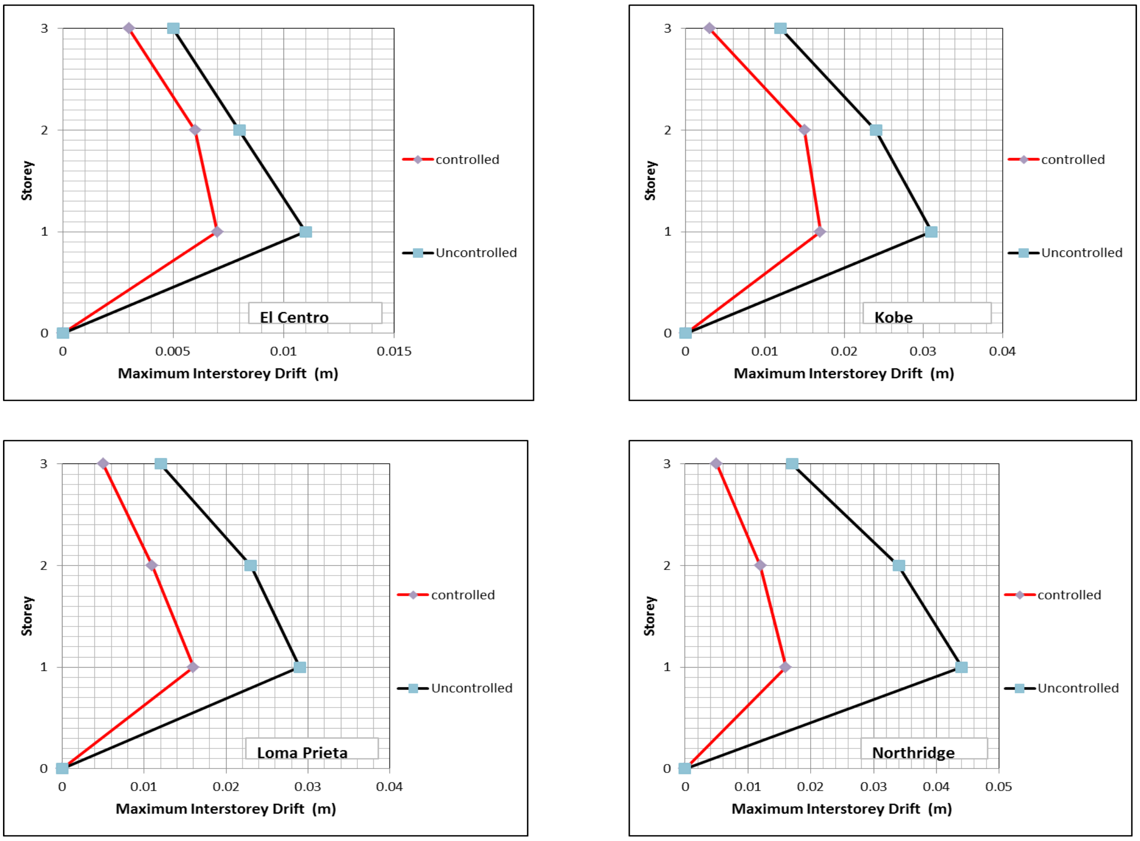

Figure 5.7: Comparison of Inter Storey Drift for Different EQ Excitation

Table 5.16: Inter Storey Drift under Northridge (PGA-1.585g) EQ Excitation

Maximum Inter Storey Drift (m)						
	1^{st}	% Red.	2^{nd}	% Red.	Roof	% Red.
Controlled	0.016	63.63	0.012	64.70	0.005	70.58
Uncontrolled	0.044	0.0	0.034	0.0	0.017	0.0

From results, it is evident that storey drift is maximum at 1^{st} storey level, so comparison of storey drift is done at level of 1^{st} storey of the structure. It is clear from graphs that storey drift is decreased by attaching friction damper to structure.For controlled building with friction damper reduction is 44.82%, 45.16%, 44.82% and 63.63% in inter storey drift is observed,for El Centro, Kobe, Loma Prieta and Northridge earthquake excitations, respectively, with respect to uncontrolled structure.Maximum reduction is archived for Northridge earthquake excitation.From this results it is observed that, reduction in inter storey drift up to 44% to 64% is achieved using friction damper with co-efficient of damping 'C_d'=1244 $kN \cdot sec/cm$ is used, under four different types of earthquake excitations.

5.3 Summary

This chapter deals with the response of the three storey shear building using friction damper by numerical method like Newmark-Beta for four different types of earthquake excitations through MATLAB. Response quantities of uncontrolled building like relative displacement, relative velocity, and absolute acceleration are compared with the controlled building. Results obtained has shown that friction damper is quit effective to reduce the all response quantities about more than 50 % for damping co-efficient 'C_d' value 1244 $kN \cdot sec/cm$.

Chapter 6

Response of Building using MR Damper

6.1 General

This chapter deals with the response of three storey shear building using Magneto-Rheological damper. Numerical method Rungge-Kutta is used to find out the response quantity of controlled structure. Results of different response quantities are given in subsequent sections.

6.2 Design of MR Damper

To understand the influence of MR Damper (MR), a three storey shear building has been considered as given in section 4.2, which was converted into a lump mass model. From this lump mass model of building without damper, mass matrix, stiffness matrix and damping matrix is determined, which is given Appendix-A. For response of controlled building, a MR damper is connected rigidly at the first storey. A diagram of MR damper implementation is shown in Figure 3.12. The equations of motion of the structure are given by where is the measured control force, defined by f. The structural measurements used for calculating the desired control force include the absolute accelerations of the three floors of the structure, and the displacement of the

MR damper. The MR damper parameters given are used for the simulation studies, except that an appropriate translation of coordinates is made to cancel the initial offset caused by the accumulator in the MR damper (i.e., x_0 was set at zero). The essential effect was to eliminate the need to consider asymmetry in the results.
In this study, two cases are considered in which the MR damper is employed in a passive mode. In the first case, designated passive-off, the command voltage to the MR damper is held at 0 V. The second passive case the voltage to the MR damper is held at the maximum voltage level (2.25 V) and is denoted as passive-on. The results for these two cases indicate that both of the passive systems are able to achieve a reasonable level of performance.

6.3 Results and Discussion

This section presents the results obtained through numerical method Runge-Kutta of three storey R.C. frame building with MR damper. The response of R.C frame building in the form of relative displacement, relative velocity and absolute acceleration. Efficiency of these systems is investigated for four earthquake excitation of different peak acceleration value, namely El Centro, Kobe, Loma Prieta and Northridge. The undamped structural response was found out as discussed in Section 4.6 of chapter 4 in order to compare its results with the results of the building embedded with MR Damper. There are various ways of assessing seismic response, but computation of top storey response is a reasonable measure of the overall effect of seismic response. The reduction in the top storey velocity and acceleration at first storey of the building are also investigated for four types of earthquake excitations.

6.3.1 Comparison of Displacement Response

The results of displacement response of uncontrolled and controlled building for four earthquake excitation of different peak acceleration value, namely El Centro, Kobe, Loma Prieta and Northridge are given in Table 5.1 to 5.4 respectively. The graphical representations of comparison of displacement response for uncontrolled and controlled structure are presented in Figure 5.2. From results, it is evident that displacement of top storey is highest, so comparison of displacement is done at top of the building.

Table 6.1: Relative Displacement under El Centro (PGA-0.3129g) EQ Excitation

Maximum Storey Displacement (m)						
	1^{st}	% Red.	2^{nd}	% Red.	Roof	% Red.
Passive On	0.0079	24.03	0.0140	23.91	0.0166	27.51
Passive Off	0.0102	1.92	0.0181	1.63	0.0227	0.873
Uncontrolled	0.0104	0.0	0.0184	0.0	0.0229	0.0

Table 6.2: Relative Displacement under Kobe (PGA-0.6936g) EQ Excitation

Maximum Storey Displacement (m)						
	1^{st}	% Red.	2^{nd}	% Red.	Roof	% Red.
Passive On	0.0231	25.24	0.0420	23.07	0.0521	21.41
Passive Off	0.0301	2.58	0.0532	4.21	0.0649	2.11
Uncontrolled	0.0309	0.0	0.0546	0.0	0.0663	0.0

Table 6.3: Relative Displacement under Lomaprieta (PGA-0.6437g) EQ Excitation

Maximum Storey Displacement (m)						
	1^{st}	% Red.	2^{nd}	% Red.	Roof	% Red.
Passive On	0.0232	19.44	0.0421	17.45	0.0517	17.28
Passive Off	0.0277	3.82	0.0498	2.35	0.0421	3.04
Uncontrolled	0.0288	0.0	0.0510	0.0	0.0625	0.0

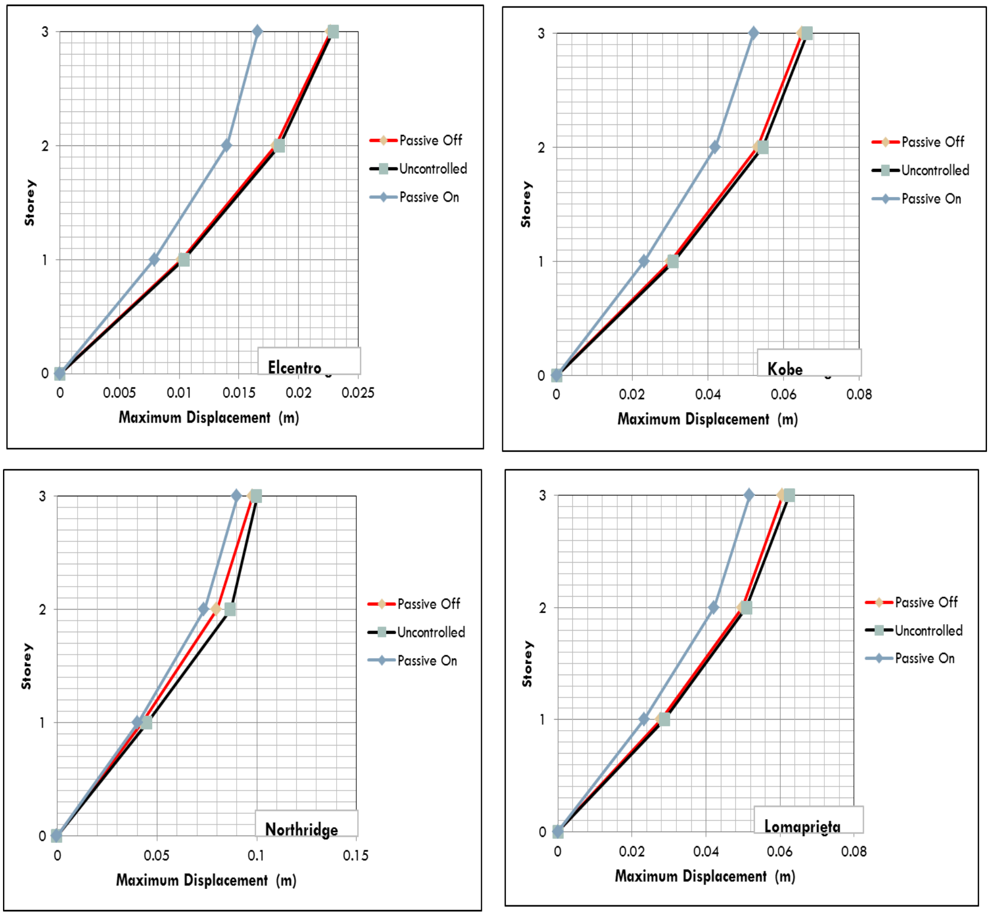

Figure 6.1: Comparison of Displacement for Different EQ Excitation

Table 6.4: Relative Displacement under Northridge (PGA-1.585g) EQ Excitation

Maximum Storey Displacement (m)						
	1^{st}	% Red.	2^{nd}	% Red.	Roof	% Red.
Passive On	0.0405	10.00	0.0738	15.26	0.0903	9.88
Passive Off	0.0427	5.32	0.0801	1.80	0.0981	2.09
Uncontrolled	0.0451	0.0	0.871	0.0	0.1002	0.0

There are two cases considered for MR damper i.e. Passive Off and Passive On respectively. In passive off case applied to damper is 0 V and 2.25 V for passive on case. It is very clear from the figure that in case of passive off very less reduction is achieved as compare to passive on case. 3.04 % reduction for Lomaprieta earthquake in case of passive off and 27.51 % is achieved for El centro earthquake in case of passive on case. Very less reduction is achieved in case of passive off case for El centro earthquake and for passive on case very less reduction in archived for Northridge earthquake.

6.3.2 Comparison of Velocity Response

Results of the maximum storey velocity of building obtained under four earthquake excitation, namely El Centro, Kobe, Loma Prieta and Northridge are presented in figure. It is quite clear that velocity at roof level is highest among all storey.

Table 6.5: Relative Velocity under El Centro (PGA-0.3129g) EQ Excitation

Maximum Storey Velocity (m/sec)						
	1^{st}	% Red.	2^{nd}	% Red.	Roof	% Red.
Passive On	0.155	20.51	0.247	24.00	0.341	13.01
Passive Off	0.191	2.05	0.325	1.53	0.387	1.27
Uncontrolled	0.195	0.0	0.325	0.0	0.392	0.0

Table 6.6: Relative Velocity under Kobe (PGA-0.6936g) EQ Excitation

Maximum Storey Velocity (m/sec)						
	1^{st}	% Red.	2^{nd}	% Red.	Roof	% Red.
Passive On	0.425	17.31	0.636	25.96	0.694	30.39
Passive Off	0.501	2.52	0.832	3.14	0.964	3.30
Uncontrolled	0.514	0.0	0.859	0.0	0.997	0.0

Table 6.7: Relative Velocity under Lomaprieta (PGA-0.6437g) EQ Excitation

Maximum Storey Velocity (m/sec)						
	1^{st}	% Red.	2^{nd}	% Red.	Roof	% Red.
Passive On	0.446	25.24	0.787	21.97	1.030	17.76
Passive Off	0.5388	2.63	0.978	3.08	1.216	2.91
Uncontrolled	0.553	0.0	1.009	0.0	1.252	0.0

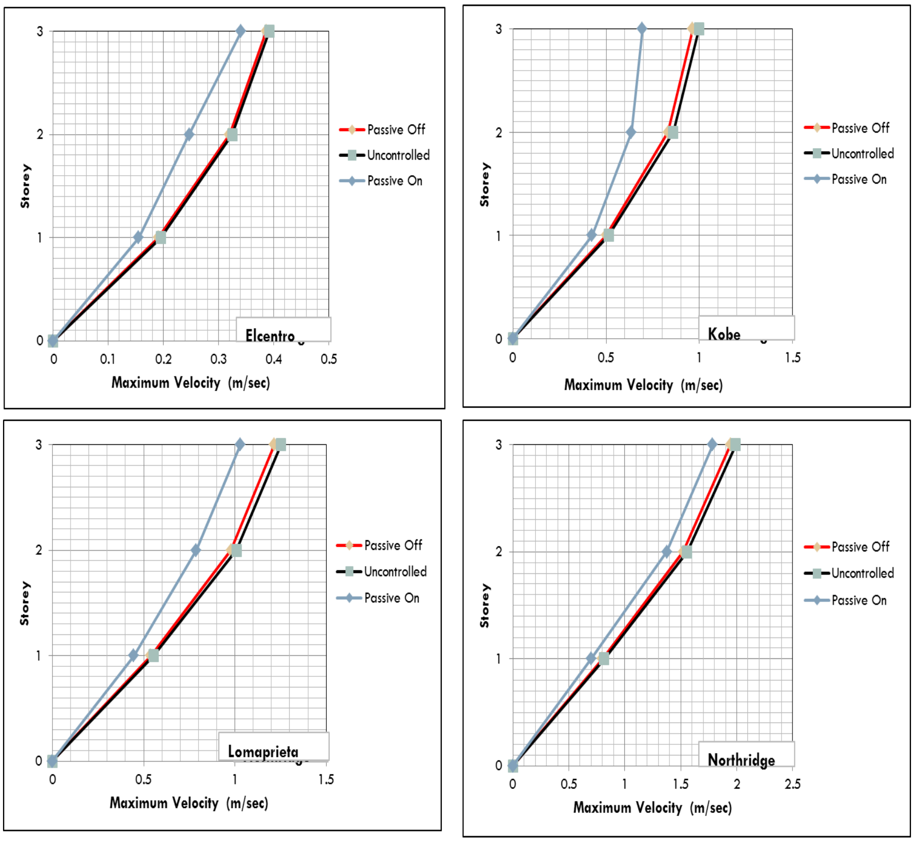

Figure 6.2: Comparison of Velocity for Different EQ Excitation

Table 6.8: Relative Velocity under Northridge (PGA-1.585g) EQ Excitation

Maximum Storey Velocity (m/sec)						
	1^{st}	% Red.	2^{nd}	% Red.	Roof	% Red.
Passive On	0.700	14.17	1.377	11.61	1.784	11.54
Passive Off	0.799	2.08	1.523	2.24	1.944	2.31
Uncontrolled	0.816	0.0	1.558	0.0	1.994	0.0

From result, it is very clear that maximum reduction is achieved 3.30 % and 30.39 % for passive off and passive on case for Kobe earthquake.

6.3.3 Comparison of Acceleration Response

Figure shows the maximum value of storey acceleration of building under the four earthquake excitation for uncontrolled and controlled building, equipped with MR damper at ground floor.

Table 6.9: Absolute Acceleration under El Centro (PGA-0.3129g) EQ Excitation

Maximum Storey Acceleration (m/sec^2)						
	1^{st}	% Red.	2^{nd}	% Red.	Roof	% Red.
Passive On	4.870	11.75	6.019	3.82	6.495	22.89
Passive Off	5.315	3.69	6.166	1.47	8.084	4.03
Uncontrolled	5.519	0.0	6.258	0.0	8.424	0.0

Table 6.10: Absolute Acceleration under Kobe (PGA-0.6936g) EQ Excitation

Maximum Storey Acceleration (m/sec^2)						
	1^{st}	% Red.	2^{nd}	% Red.	Roof	% Red.
Passive On	11.02	0.18	13.82	21.11	18.23	13.51
Passive Off	10.83	1.90	17.07	2.56	20.61	2.22
Uncontrolled	11.04	0.0	17.52	0.0	21.08	0.0

Table 6.11: Absolute Acceleration under Loma Prieta (PGA-0.6437g) EQ Excitation

Maximum Storey Acceleration (m/sec^2)						
	1^{st}	% Red.	2^{nd}	% Red.	Roof	% Red.
Passive On	9.938	3.178	14.792	12.098	17.514	17.18
Passive Off	10.181	0.808	16.309	3.170	20.518	2.9
Uncontrolled	10.264	0.0	16.828	0.0	21.148	0.0

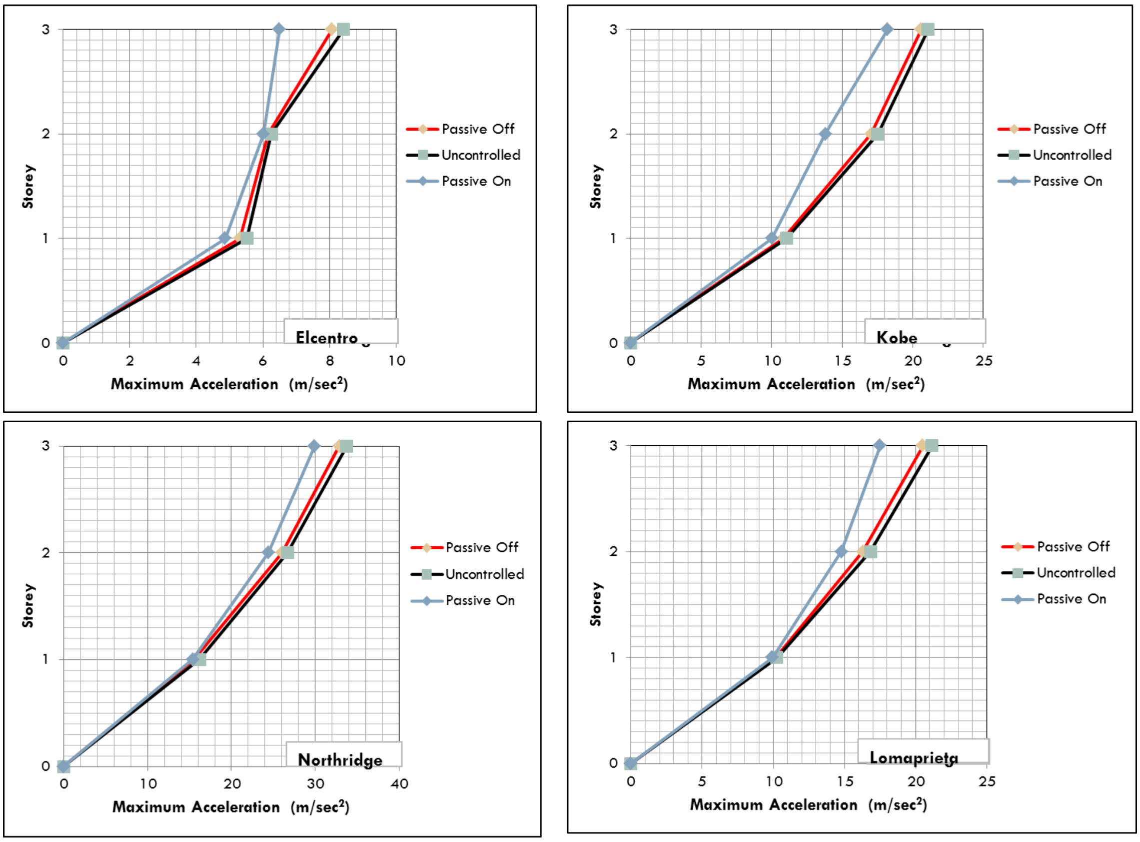

Figure 6.3: Comparison of Acceleration for Different EQ Excitation

Table 6.12: Absolute Acceleration under Northridge (PGA-1.585g) EQ Excitation

Maximum Storey Acceleration (m/sec^2)						
	1^{st}	% Red.	2^{nd}	% Red.	Roof	% Red.
Passive On	15.38	5.03	24.39	8.58	29.88	11.38
Passive Off	15.55	3.95	26.03	2.43	32.84	2.60
Uncontrolled	16.19	0.0	26.68	0.0	33.84	0.0

Maximum reduction is achieved for Elcentro earthquake i.e. 4.036 % and 22.898 % in case of passive off and passive on respectively when building is equipped with MR damper of 1000 kN at ground floor.

6.3.4 Comparison of Interstorey Response

For the reason of effective damage control and safety measure of the structures, code IS 1893:2002 specified the upper limit of the storey drift as a 0.004 H where, H is the storey height. Inter storey drift obtained from uncontrolled and controlled structure are given in Table 7.13 to 7.16

Table 6.13: Inter Storey Drift under El Centro (PGA-0.3129g) EQ Excitation

Maximum Inter Storey Drift (m)						
	1^{st}	% Red.	2^{nd}	% Red.	Roof	% Red.
Passive On	0.0079	24.08	0.0061	23.75	0.0026	42.22
Passive Off	0.0102	1.92	0.0079	1.25	0.0046	-2.22
Uncontrolled	0.0104	0.0	0.0080	0.0	0.0045	0.0

Table 6.14: Inter Storey Drift under Kobe (PGA-0.6936g) EQ Excitation

Maximum Inter Storey Drift (m)						
	1^{st}	% Red.	2^{nd}	% Red.	Roof	% Red.
Passive On	0.0231	25.24	0.0189	20.25	0.0101	13.67
Passive Off	0.0301	2.58	0.0231	2.53	0.0117	0.0
Uncontrolled	0.0309	0.0	0.0237	0.0	0.0117	0.0

Table 6.15: Inter Storey Drift under Lomaprieta (PGA-0.6437g) EQ Excitation

Maximum Inter Storey Drift (m)						
	1^{st}	% Red.	2^{nd}	% Red.	Roof	% Red.
Passive On	0.0232	19.44	0.0189	14.86	0.0096	16.52
Passive Off	0.0278	3.47	0.0222	0.00	0.0109	5.21
Uncontrolled	0.0288	0.0	0.0222	0.0	0.0115	0.0

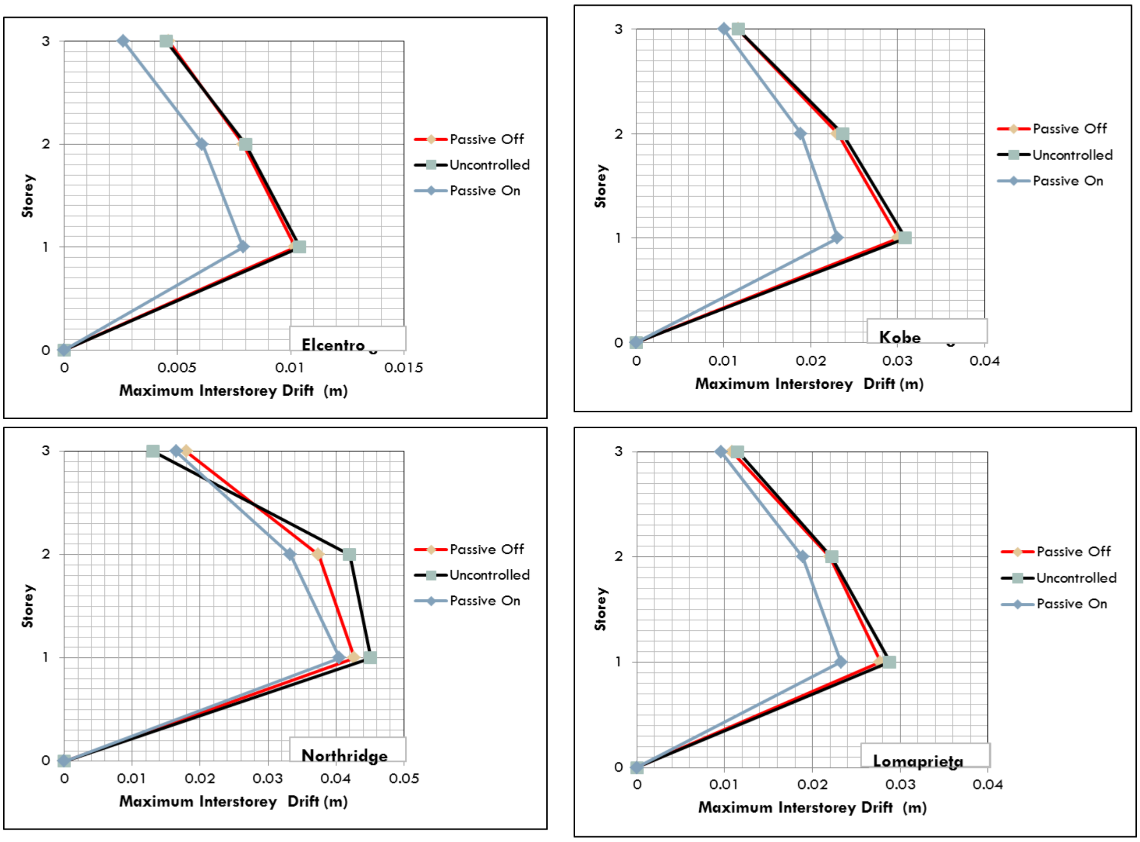

Figure 6.4: Comparison of Inter Storey Drift for Different EQ Excitation

Table 6.16: Inter Storey Drift under Northridge (PGA-1.585g) EQ Excitation

Maximum Inter Storey Drift (m)						
	1^{st}	% Red.	2^{nd}	% Red.	Roof	% Red.
Passive On	0.0405	10.19	0.0333	20.71	0.0165	-25.95
Passive Off	0.0427	5.32	0.0374	10.95	0.0180	-37.40
Uncontrolled	0.0451	0.0	0.042	0.0	0.0131	0.0

From figure it is observed that maximum reduction is achieved for Kobe earthquake i.e. 2.58 % for passive off case and 25.24 % in passive on case respectively.

6.4 Summary

A new semi-active control device called a MR damper, was evaluated for use in structural response reduction to seismic loads. Because of its mechanical simplicity, low operating power requirements, environmental robust-ness, and demonstrated potential for developing forces sufficient for full-scale applications, it is a particularly promising device for structural response reduction.Response quantities of uncontrolled building like relative displacement, relative velocity, and absolute acceleration are compared with the controlled building for.This chapter deals with the response of the three storey shear building using MR damper by numerical method Runnge-Kutta for Northridge type of earthquake excitations through MATLAB. From table it can be said that when voltage is applied to the MR damper i.e passive on mode is more effective as compare to passive off mode.

Chapter 7

Comparisons of Passive Control Devices

7.1 General

The chapter deals with the response of three storey shear building using different passive devices. All the devices are connected between ground and first storey. Results of different response quantities are given in subsequent sections.

7.1.1 Comparison of Displacement Response

Figure **??**.1are shows the response quantity of uncontrolled and controlled building under the El cento, Kobe, Loma Prieta, and Northridge earthquake respectively. From results, it is evident that displacement of top storey is highest, so comparison of displacement is done at top of the structure for all devices.

For controlled building with added damping and stiffness (ADAS) damper maximum reduction of 66.9% in roof displacement is observed, when Stiffness Ratio 'SR' is equal to 2 for Northridge earthquake excitation respectively, with respect to uncontrolled structure.For all earthquake ADAS damper is very effective in reducing maximum displacement. It can be seen from the figure that MR damper reduces very less response as compare to all other type of damper.

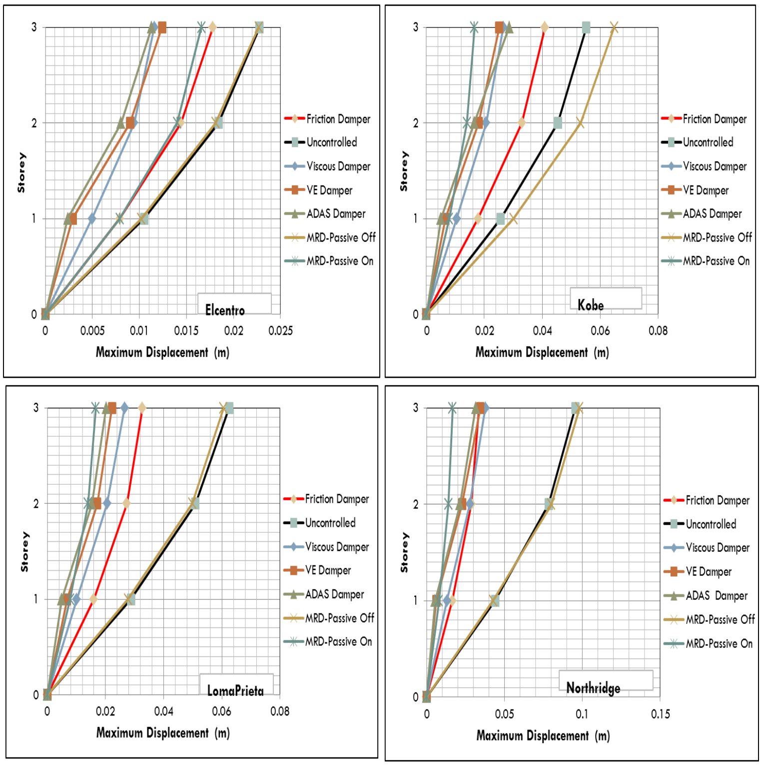

Figure 7.1: Comparison of Storey Displacement under Four EQ Excitation

7.1.2 Comparison of Velocity Response

Results of the maximum storey velocity of building obtained under four earthquake excitation, namely El Centro, Kobe, Loma Prieta and Northridge are presented in figure

From results, controlled building with friction damper reduction of 69.17% in maximum roof velocity is observed, for El Northridge earthquake excitation respectively, with respect to uncontrolled structure that is maximum % of reduction to other type of passive devices.

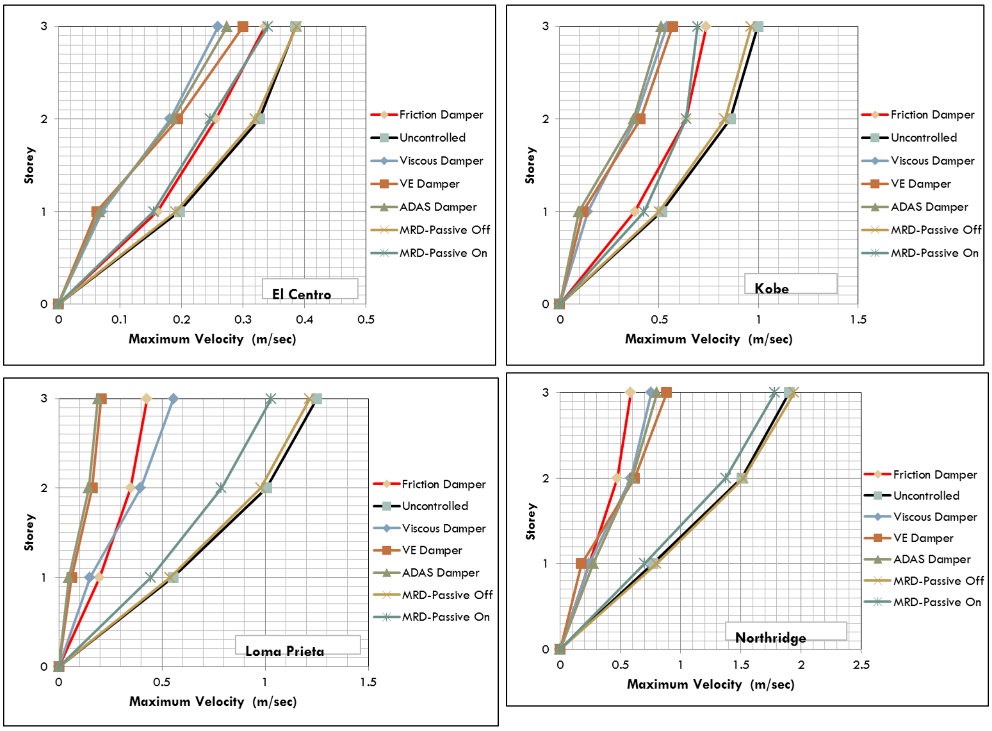

Figure 7.2: Comparison of Storey Velocity under Four EQ Excitation

7.1.3 Comparison of Acceleration Response

Figure 7.3 shows the maximum value of storey acceleration of building under the four earthquake excitation for uncontrolled and different type of passive devices added structure.

For Loma Prieta earthquake, significant roof acceleration reduction is achieved as compare to other earthquake. For controlled building with friction damper reduction of 66.78% in roof acceleration is observed, when 'Cd'(Coefficient of damping) is equal to 1244 kN sec/m for Loma Prieta earthquake excitation, with respect to uncontrolled structure.

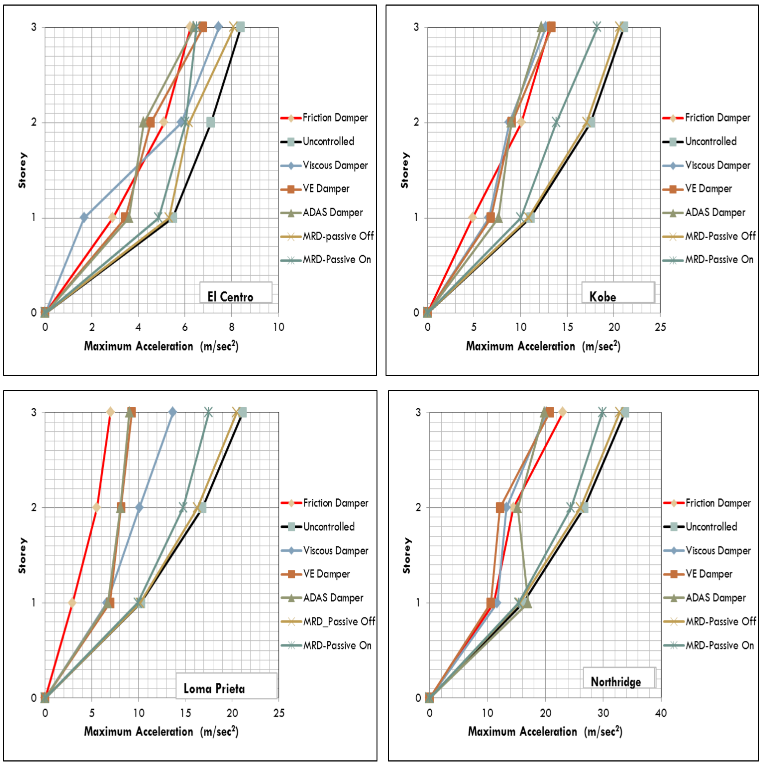

Figure 7.3: Comparison of Storey Acceleration under Four EQ Excitation

7.1.4 Comparison of Inter Storey Drift

For the reason of effective damage control and safety measure of the structures, code IS 1893:2002 specified the upper limit of the storey drift as a 0.004 H where, H is the storey height. Inter storey drift for uncontrolled and controlled with four different type of passive devices is shown in figure.

From results, it is evident that inter storey drift is maximum at 2^{nd} storey level, so comparison of inter storey drift is done at level of 2^{nd} storey of the building. It is clear from results that inter storey drift is constantly decreased by attaching ADAS damper to structure but maximum reduction is achieved by friction damper as 75% and 70% for Kobe and Northridge earthqauke.

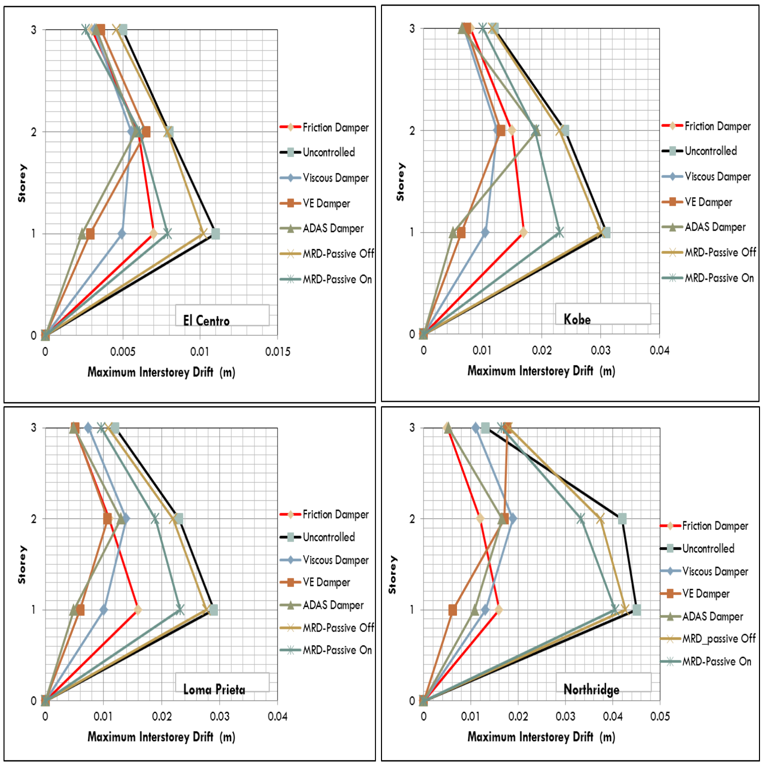

Figure 7.4: Comparison of Storey Inter Storey Drift under Four EQ Excitation

7.2 Summary

This chapter deals with the comparison of shear building using four different damper under the EL Centro, Kobe, Loma Prieta, and Northridge earthquake excitations through MATLAB. From the results it is observed that friction damper is quite better than other passive devices. ADAS damper is efficient in reducing maximum displacement. Friction is better in reducing maximum velocity, acceleration and interstorey drift.

Chapter 8

Summary and Conclusions

8.1 Summary

Seismic protective systems are used apart from buildings design with conventional seismic design, such that they remain practically undamaged during severe earthquake. When strong earthquake motions come, the inherent damping in the structure is not sufficient to mitigate the structural response, therefore extra damping is required in the form of energy dissipating systems. Three basic technologies are used to protect buildings from damaging earthquake effects. These are Base Isolation, Passive Energy Dissipation Devices and Active Control Devices. In passive energy dissipation systems the motion of structure is controlled by adding devices to structure in the form of stiffness, mass and damping.

In this work, the main focuses was on the passive energy dissipation devices like, friction and MR dampers. Though MR Damper is semi-active device but in present study it is considered as passive device. To understand the behavior of friction and MR damper, characterization of this dampers have been carried out under the sinusoidal and different earthquake excitations, namely El Centro, Kobe, Loma Prieta, and Northridge excitations.

A three storey shear building has been considered. This building is converted to lump mass model and, mass matrix and stiffness matrix are derived. A rayleigh's damping is assumed and damping matrix are obtained. Equation of motion for multi degree of freedom system subjected to earthquake excitations are derived. Also, equation of motion for shear building equipped with passive devices like friction and MR dampers are derived. These equation of motions are solved using numerical method like Newmark-Beta and Rungge-Kutta for uncontrolled and controlled building under the different earthquake excitations through MATLAB. Response quantities like maximum displacement, maximum velocity, maximum acceleration and maximum inter storey drift has been obtained for uncontrolled and controlled building. These response quantities of uncontrolled building has been compared with the controlled building.

8.2 Conclusions

The main aim of the work was to check the effectiveness of passive devices and the mathematical model and behavior of friction and MR damper. From mathematical model of friction and MR Damper has been carried out under the sinusoidal and random earthquake excitations. Three storey shear building analysis has been done using time stepping numerical method Newmark-Beta and Runge-Kutta for uncontrolled and the building equipped with passive energy dissipation devices, and extract the response quantities like maximum storey displacement, velocity, acceleration and damper force for four earthquake excitations through MATLAB.
Based on the work carried out following conclusions are made.

- Numerical results of three storey shear building equipped with friction damper clearly indicate that the maximum roof displacement, maximum roof velocity, maximum roof acceleration and maximum inter storey drift are significantly reduces as co-efficient of damper 'C_d' increases, under four different types of earthquake excitations.

    a. Maximum roof displacements are reduced by 64.67 % under the Northridge earthquake excitation when damping co-efficient is 1244 $kNsec/cm$.

b. Maximum roof velocity are reduced by 69.17 % under the Loma Prieta earthquake excitation when damping co-efficient is 1244 $kNsec/cm$.

c. Maximum roof acceleration are reduced by 66.78 % under the Loma Prieta earthquake excitation when damping co-efficient is 1244 $kNsec/cm$.

d. Maximum inter storey drift at first storey are reduced by 75 % under the Kobe earthquake when damping co-efficient is 1244 $kNsec/cm$.

e. This result indicates that amount of damping directly influence the responses by reducing it.

a. It can also be concluded that MR damper are effective in reducing all response quantities of building. Two cases where considered as 'passive off' and 'passive on' using 1000 kN MR damper.

b. Maximum roof displacements are reduced by 3.04 % in case of Passive Off case and in case of Passive On 27.51 % is reduced under the Lomaprieta and Elcentro earthquake excitations respectively when 1000 kN MR Damper is used

c. Maximum roof velocity are reduced by 3.30 % in case of Passive Off case and in case of Passive On 30.39 % is reduced under the Kobe earthquake excitation when 1000 kN MR Damper is used.

d. Maximum roof acceleration are reduced by 4.036 % in case of Passive Off case and in case of Passive On 22.898 % under the Northridge earthquake excitation when 1000 kN MR Damper is used.

e. Maximum damper force is 86.89 kN for Passive Off case and 432.44 kN for Passive On case for Northridge earthquake.

- It is found from the results of three storey shear building equipped with added damping and stiffness damper (ADAS) and friction damper and friction damper are more effective in reducing the response quantity as compare to all other type of damping devices.

- From all the results of different passive damper added three storey shear building, it is concluded that all are good enough to reduces all response quantities. It can be also concluded that friction damper are more effective under the Northridge type of earthquake excitations, however ADAS damper is suitable for Loma Prieta type of earthquake excitations.

8.3 Future Scope of the Work

The present work can be used as an input for further work explained as follows.

- In this study three storey building with passive devices equipped at first storey is considered, however the effectiveness of more passive dampers placed at different storey can be studied.
- Different passive devices (i.e Active and Semi-Active) can also be used for the response of building.
- Use of MR damper as a semi-active device device can be done.
- The optimal locations of damper placement can be obtained through various optimization techniques.
- More number of earthquake time history can be used for finding response.
- Comparative study of cost analysis of different passive energy dissipation devices can help in appropriate selection of proper damper for various buildings in various seismic excitations.

Appendix A

Calculation of Eigenvalue and Eigenvector

As discussed earlier, three storey shear building is shown in Figure 4.1 is converted in to a Lump mass model, which is given in Figure 4.2. Calculation of Eigenvalues, Eigenvectors, Mass Matrix [M], Stiffness Matrix [K], Damping Matrix [D] of this lump mass model are found out as follows,

Building Configuration

Number of Stories	3 No.
Floor height (c/c)	3 m
Imposed load	3 kN/m^2
Percentage of Imposed Load	0.75 kN/m^2
Characteristics Strength of Concrete, f_{ck}	25 N/mm^2
Characteristics Strength of Steel, f_y	415 N/mm^2
No. of Bays In X-Direction	3 No.
No. of Bays In Y-Direction	3 No.
Bay Width In X-Direction	4 m
Bay Width In Y-Direction	4 m

Column size,	(0.3 x 0.3) m
Beam size,	(0.23 x 0.3) m
Depth of slab	0.12 m
Specific weight of R.C.C	25 kN/m^3
Specific weight of infill	0
Inherent Damping Ratio for Concrete Structure	5%

Lump Mass Calculation

At Roof Level		At Typical Storey	
Weight of Infill	0	Weight of Infill	0
Weight of Columns	54 kN	Weight of Columns	108 kN
Weight of Beams	165.6 kN	Weight of Beams	165.6 kN
Weight of Slab	432 kN	Weight of Slab	432 kN
Imposed Load	0 (IS 1893:2002)]	Imposed Load	108 kN
Total Roof Load	651.6 kN	Total Floor Load	1627.2 kN

Total Seismic Weight of Building, W = 2278.8 kN

Calculation of Eigenvalues and Eigenvectors

Mass Matrix of lumped mass model of building, M

$$[\mathrm{M}]= \begin{vmatrix} M_1 & 0 & 0 \\ 0 & M_2 & 0 \\ 0 & 0 & M_3 \end{vmatrix} \mathrm{Kg}$$

$$[\mathrm{M}]= \begin{vmatrix} 82935.78 & 0 & 0 \\ 0 & 82935.78 & 0 \\ 0 & 0 & 66422.02 \end{vmatrix} \mathrm{Kg}$$

Stiffness Matrix of lumped mass model of building, K

Column stiffness in X and Y direction, k=12EI/l^3

Total lateral stiffness of each story = No of columns in a story × k = 120000000 N/m

$$[K]= \begin{vmatrix} K_1+K_2 & -K_2 & 0 \\ -K_2 & K_2+K_3 & -K_3 \\ 0 & -K_3 & K_3 \end{vmatrix}$$

$$[K]= \begin{vmatrix} 240000000 & -120000000 & 0 \\ -120000000 & 240000000 & -120000000 \\ 0 & -120000000 & 120000000 \end{vmatrix} \text{N/m}$$

For the above stiffness and mass matrices, eigenvalue and eigenvector are worked out using MATLAB as follows,

$$[K] \times [M]^{-1} = \begin{vmatrix} 2893.81 & -1446.9027 & 0 \\ -1446.9 & 2893.80531 & -1806.6298 \\ 0 & -1446.9027 & 1806.62983 \end{vmatrix}$$

Eigenvalues or natural frequencies of various modes are,

$$[\omega^2] = \begin{vmatrix} 320.82 & 0 & 0 \\ 0 & 2438.17 & 0 \\ 0 & 0 & 4835.25 \end{vmatrix}$$

ω_1=17.92 rad/sec, ω_2=49.38 rad/sec, ω_3=69.54 rad/sec,

The eigenvector (mode shapes) and natural periods corresponding to each natural frequency are,

$$[\phi] =[\phi_1\ \phi_2\ \phi_2] = \begin{vmatrix} 0.3364 & -0.7234 & -0.5391 \\ 0.5982 & -0.2278 & 0.7233 \\ 0.7273 & 0.6517 & -0.4315 \end{vmatrix}$$

$$T = \begin{vmatrix} 0.351 & 0 & 0 \\ 0 & 0.127 & 0 \\ 0 & 0 & 0.351 \end{vmatrix} \text{sec}$$

Evaluate the Rayleigh Damping Matrix

By considering first mass-proportional damping and stiffness-proportional damping, C = $a_0M + a_1K$
Where, C is the rayleigh damping matrix; a_0 and a_1 are the co-efficient; M and K are the mass and stiffness matrix of building respectively. The co-efficient a_0 and a_1 can be determine from specified damping ratios ξ_i and ξ_j for the i th and j th modes, respectively. If all modes are to have the same damping ratio ξ, which is reasonable based on experiment data, therefore

$$a_0 = \frac{\xi\omega_i\omega_j}{\omega_i + \omega_j}$$

$$a_1 = \frac{2\xi}{\omega_i + \omega_j}$$

Where, ξ is the inherent damping ratio of the structure, ω_i and ω_j are the i th and j th natural frequency of of the building. Therefore, damping matrix of three storey building as per rayleigh's damping 'C' is,

$$C = \begin{vmatrix} 465677.03 & -178334.3 & 0 \\ -178334.3 & 465677.027 & -178334.3 \\ 0 & -178334.3 & 265637.512 \end{vmatrix} \text{N Sec/m}$$

Appendix B

MATLAB Code

A) MATLAB Code for Response of Friction Damper Subjected to Sinusoidal Input (for varying value of frequency)

```
f=1:1:5;a=0.05;cd=28;Fc=30;w =2*3.14*f;t=0:0.01:4;x=a*sin(w*t);
x1=a*w*cos(w*t);
F=Fc*sign(x1);subplot(2,2,1:2)
plot(t,F,'r');% Plot of Force Vs Time
grid on
xlabel('Time(sec)')
ylabel('Force(N)')
hold on
subplot(2,2,3)
plot(x,F,'r');% Plot of Force Vs Displacement
grid on
xlabel('Displacement(m)')
ylabel('Force(N)')
hold on
subplot(2,2,4)
plot(x1,Fc,'r');% Plot of Force Vs Velocity
grid on
```

```
xlabel('Velocity(m/sec)')
ylabel('Force(N)')
hold on
end
```

B) MATLAB Code for Response of Friction Damper Subjected to Earthquake Excitations

```
% Plot of force vs time,force vs displacement,force vs velocity for Friction damper)
f=1:1:5;% frequency in Hz
a=0.05;%Amplitudes are varying(in m)
cd=28;% Damping co efficient in N*S/m
Fc=30;%Coulomb force in N
t=0:0.01:40;%Time in Sec
fid1 = fopen('.txt file of El Centro Displacement Data');
x=fscanf(fid1,'%g'); %Displacement in cm
x=[0;x]
x=x.*0.01
fid2=fopen(".txt file of El Centro Velocity Data');
x1=fscanf(fid2,'%g')
x1=[0;x1]
x1=x1*0.01
F=Fc*sign(x1);% Force in Damper in N
subplot(2,2,1:2)
plot(t,F,'r');% Plot of Force Vs Time
grid on
xlabel('Time(sec)')
ylabel('Force(N)')
hold on
subplot(2,2,3)
```

```
plot(x,F,'r');% Plot of Force Vs Displacement
grid on
xlabel('Displacement(m)')
ylabel('Force(N)')
hold on
subplot(2,2,4)
plot(x1,Fc,'r');% Plot of Force Vs Velocity
grid on
xlabel('Velocity(m/sec)')
ylabel('Force(N)')
hold on
```

C) MATLAB Code for Response of MR Damper Subjected to Sinusoidal Motion

```
% Code forBingham Model % Plot of force vs time,force vs displacement,force vs velocity for MR damper
f=2.5;% frequency in Hz
a=1.5;%Amplitudes are varying(in cm)
Ce=50;%Damping co efficient in N*S/cm
f0=-95;
Fm=670;% Coulomb force in N
w =2*3.14*f;% Frequency is constant in rad/sec
t=0:0.02:1;%Time in Sec
x=a*sin(w*t);
x1=a*w*cos(w*t);
F =Ce*x1+Fm*sign(x1)+f0;% Force in Damper in N
subplot(2,2,1:2)
plot(t,F);% Plot of Force Vs Time
grid on
```

```
xlabel('Time(sec)')
ylabel('Force(N)')
hold on
subplot(2,2,3)
plot(x,F);% Plot of Force Vs Displacement
grid on
xlabel('Displacement(m)')
ylabel('Force(N)')
hold on
subplot(2,2,4)
plot(x1,F);% Plot of Force Vs Velocity
grid on
xlabel('Velocity(m/sec)')
ylabel('Force(N)')
hold on
end
```

D) MATLAB Code for Response of MR Damper Subjected to Sinusoidal Motion

Main file

```
% Code for BoucWen model of MR Damper
% Defining Excitation
global amp freq wn
amp = 1.5;
freq = 2.5;
wn = 2*pi*freq;
% Define time span
t = [0:0.01:1];
% Calculating Displacement and Velocity for MR DAMPER
```

```
disp = amp*sin(wn*t);
velo = amp*wn*cos(wn*t);
table = [disp' velo']
% ploting Displacement and Velocity for MR damper subplot(2,1,1)
plot(t,disp)
ylabel('Displacement (cm)')
subplot(2,1,2)
plot(t,velo)
xlabel('TIme (s)')
ylabel('Velocity (cm/s)')
% Solving Differential equation for evolutionary veriable 'z' for MR DAMPER
z=0;
options=odeset('reltol',1e-6,'abstol',1e-8,'stats','on');
[t, z]=ode45('diffeqnz',t,z)
plot(t,z)
xlabel('Time (s)')
ylabel('Evolutionary Variable z')
c0=50; k0=25; x0=3.8; ALFA=880;
Force=c0*velo' + k0*(disp'-x0) + ALFA*z
table = [t z disp' velo' Force]
% Ploting response of MR Damper
subplot (2,1,1)
plot(t,Force,'r')
grid
xlabel('Time (Sec)')
ylabel('Force (N)')
subplot (2,2,3)
plot(disp,Force,'r')
grid
xlabel('Displacement (cm)')
```

```
ylabel('Force (N)')
subplot (2,2,4)
plot(velo,Force,'r')
grid
xlabel('Velocity (cm/sec)')
ylabel('Force (N)')
Function File
function zdot = diffeqnz(t,z)
global amp freq wn
G=100; B=100; A=120;
disp = amp*sin(wn*t);
velo = amp*wn*cos(wn*t);
zdot=(-G*abs(velo)*z*abs(z) - B*(velo)*(abs(z)^2) + A*(velo));
```

E) MATLAB Code for Seismic Response of Uncontrolled Building to Find out Maximum Roof Displacement, Velocity and Acceleration using Newmark-Beta Method (El Centro EQ Excitation)

```
%Seismic Response of Three storey uncontrolled Building using newmark-Beta method
(El centro) clc;
close all
%mass matrix
m=[82935.78 0 0;0 82935.78 0;0 0 66422.02];
disp('mass matrix')
m
[ns,ms] = size(m);
fid=fopen('.txt file of El Centro Acceleration Data');
di = fscanf(fid,'%g');
di=[0 ; di];
di=di.*9.81; %in m/sec^2
```

```
for i=1:ns
f(:,i)=-di*m(i,i);
end
%damping matrix in N sec/m
c=[465677.0273 -178334.295 0;-178334.295 465677.0273 -178334.295;0 -178334.295 265637.5122];
disp('damping matrix')
c
%stiffness matrix in N/m
k=[240000000 -120000000 0;-120000000 240000000 -120000000;0 -120000000 120000000];
k
kim=inv(m)*k;
for i=1:ns
omega(i)=sqrt(ev(i,i));
end
disp('natural frequency')
omega
%specify integration parameter for constant acceleration method
beta=1/4;
gamma=0.5;
%specify increment in time
dt=0.01;
%specify initial displacement
u0=[0 0 0];
v0=[0 0 0];
for i=1:ns
a0=inv(m)*(f(1,:)'-c*v0'-k*u0');
end
kba=k+(gamma/(beta*dt))*c+(1/(beta*dt*dt))*m;
kin=inv(kba);
aa=(1/(beta*dt))*m+(gamma/beta)*c;
```

```
bb=(1/(2*beta))*m+dt*(gamma/(2*beta)-1)*c;
u(1,:)=u0;
v(1,:)=v0;
a(1,:)=a0;
for i=2:4001
df(i,:)=f(i,:)-f(i-1,:)+v(i-1,:)*aa'+a(i-1,:)*bb';
du(i,:)=df(i,:)*kin;
dv(i,:)=(gamma/(beta*dt))*du(i,:)-(gamma/beta)*v(i-1,:)+dt*(1-gamma/(2*beta))*a(i-
1,:);
da(i,:)=(1/(beta*dt^2))*du(i,:)-(1/(beta*dt))*v(i-1,:)-(1/(2*beta))*a(i-1,:);
u(i,:)=u(i-1,:)+du(i,:);
v(i,:)=v(i-1,:)+dv(i,:);
a(i,:)=a(i-1,:)+da(i,:);
end
tt=linspace(0,40,4001);
%find total acceleration
at3 = a(:,3) + di;
at2 = a(:,2) + di;
at1 = a(:,1) + di;
subplot(3,1,1)
plot(tt,u(:,3),'k');
xlabel('Time(sec)');
ylabel('Roof Disp.(m)');
title('Displacement Response at Roof');
subplot(3,1,2)
plot(tt,v(:,3),'k');
xlabel('Time(Sec)');
ylabel('Roof Velo.(m/sec)');
title(' Velocity Response at Roof');
subplot(3,1,3)
```

plot(tt,at3,'k');
xlabel('Time(sec)');
ylabel('Roof Accel.(m/sec^2)');
title('Acceleration Response at Roof');

F) MATLAB Code for Seismic Response of Building Equipped with Friction Damper (for C_d = 1244 kN s/m) to Find out Maximum Roof Displacement, Velocity and Acceleration using Newmark-Beta Method (El Centro EQ Excitation)

clc;
close all
%mass matrix m=[82935.78 0 0;0 82935.78 0;0 0 66422.02];
disp('mass matrix')
m
$[ns, ms] = size(m)$;
fid=fopen('.txt file of El Centro Acceleration Data');
di = fscanf(fid,'%g');
di=di.*9.81; %in m/sec^2
di=[0 ; di];
for i=1:ns
f(:,i)=-di*m(i,i);
end
%damping matrix in N sec/m
cs=[465677.0273 -178334.295 0;-178334.295 465677.0273 -178334.295;0 -178334.295 265637.5122];
disp('damping matrix')
cs
%stiffness matrix in N/m
k=[240000000 -120000000 0;-120000000 240000000 -120000000;0 -120000000 120000000];

```
k
%column vector of ones
l=[1 1 1];
%Matrix determined by the placement of VE dampers in the structure
b=[1 0 0]';
%damping matrix due to viscous damper in N sec/m
cd=[1244000 0 0;0 0 0;0 0 0];
c=cs+cd;
format long;
kim=inv(m)*k;
for i=1:ns
omega(i)=sqrt(ev(i,i));
end
disp('natural frequency')
omega
%specify integration parameter for constant acceleration method
beta=1/4;
gamma=0.5;
%specify increment in time
dt=0.01;
%specify initial displacement
u0=[0 0 0];
v0=[0 0 0];
for i=1:ns
a0=inv(m)*((f(1,:)*l'-c*v0'-k*u0'));
end
kba=k+(gamma/(beta*dt))*c+(1/(beta*dt*dt))*m;
kin=inv(kba);
aa=(1/(beta*dt))*m+(gamma/beta)*c;
bb=(1/(2*beta))*m+dt*(gamma/(2*beta)-1)*c;
```

```
u(1,:)=u0;
v(1,:)=v0;
a(1,:)=a0;
for i=2:4001
df(i,:)=f(i,:)-f(i-1,:)+v(i-1,:)*aa'+a(i-1,:)*bb';
du(i,:)=df(i,:)*kin;
dv(i,:)=(gamma/(beta*dt))*du(i,:)-(gamma/beta)*v(i-1,:)+dt*(1-gamma/(2*beta))*a(i-
1,:);
da(i,:)=(1/(beta*dt^2))*du(i,:)-(1/(beta*dt))*v(i-1,:)-(1/(2*beta))*a(i-1,:);
u(i,:)=u(i-1,:)+du(i,:);
v(i,:)=v(i-1,:)+dv(i,:);
a(i,:)=a(i-1,:)+da(i,:);
end
tt=linspace(0,40,4001);
at3 = a(:,3) + di;%total acceleration
subplot(3,1,1)
plot(tt,u(:,3),'k');
xlabel('Time(sec)');
ylabel('Roof Disp.(m)');
title('Displacement Response at Roof');
subplot(3,1,2)
plot(tt,v(:,3),'k');
xlabel('Time(Sec)');
ylabel('Roof Velo.(m/sec)');
title('Velocity Response at Roof');
subplot(3,1,3)
plot(tt,a(:,3),'k');
xlabel('Time(sec)');
ylabel('Roof Accel.(m/sec^2)');
title('Acceleration Response at Roof');
```

Appendix C

List of Paper Communicated

- Nelson N. Macwan and Dr Sharad P. Purohit, " EFFECTIVENESS OF FRICTION DAMPER FOR SEISMIC RESPONSE OF BUILDING", 3^{rd} International Conference(NUiCONE), Nirma University, Ahmedabad, India, December 2012.

References

[1] M. Abdel-Rohman and H.H. Leipholz. Active control of flexible structures. *Journal of the Structural Division*, (Vol. 104), 1978.

[2] M. Abdel-Rohman and H.H. Leipholz. Active control of tall buildings. *Journal of the Structural Division*, (Vol:109), 1983.

[3] Z. Akbay and H.M. Aktan. Intelligent energy dissipation devices. pages 427–435, 1990.

[4] Catanzarite D.M. Carlson, J.D. and K.A. St. Clair. Commercial magneto-rheological fluid devices. *5th International Conference on ER Fluids, MR Fluids and Associated Technology*, 1995.

[5] J. Chang and T.T. Soong. Journal of the engineering mechanics division. *Internatinal Conference on Building and Construction*, (Vol:106(6)):1091–1098, 1980.

[6] A. K. Chopra. Dynamics of structures. theory and appliction to earthquake engineering. *Pearson Education, Inc.*, 2007.

[7] Reinhorn A.M. Chung, L.L. and T.T. Soong. Experiments on active control of seismic structures. *Journal of Engineering Mechanics*, (Vol:114):241–256, 1988.

[8] T.T. Soong & M.C. Constantinou. Passive and active structural vibration control in civil engineering. *Vienna and new york: Springer-Verlag*, 1994.

[9] B.F. Spencer Jr. M.K. Sain Dyke, S.J. and J.D. Carlson. Seismic response reduction using magnetorheological dampers. page 145150, 1996.

[10] Soong T.T. Fujino, Y. and B.F. Spencer Jr. Structural control: Basic concepts and applications. (Vol:2), 1996.

[11] T. K. Caughey R. E. Skelton T. T. Soong B. F. Spencer J. P. Yao. G. W. Housner, L. A. Bergman. Structural control: past, present, and future. *Journal of Engineering Mechanics*, (Vol:123):897–971, 1997.

[12] T. Kobori. Future direction on research and development of seismic-response-controlled structure. 1994.

[13] Murata T. Tanida K. Kobori T. Ishii K. Koike, Y. and Y. Takenaka. Development of v-shaped hybrid mass damper and its application to high-rise buildings. 1994.

[14] N.H. McClamroch and H.P. Gavin. Intelligent energy dissipation devices. page 41734177, 1995.

[15] N. M. Newmark. A method of computation for structural dynamics. *ASCE Journol of Engineering Mechanics Division*, (Vol:85), 1959.

[16] A. S. Pall and C. Marsh. Friction damped concrete shear walls. *American Concrete Institute*, page 145150, 1981.

[17] Soong T.T. Reinhorn, A.M. and C.Y. Wen. Base isolated structures with ac-tive control. 1987.

[18] Soong T.T. Fukao Y. Lin R.C. Wang Y.P. Reinhorn, A.M. and Nakai. Experiments on active structural control under seismic loads. *Proceedings of ICOSSAR*, 1989.

[19] J. Roorda. Tendon control in tall buildings. *Journal of the Structural Division*, (Vol. 101(3)), 1975.

[20] Amazaki S. Full scale investigation of performance of tuned active dampers installed in landmark tower in yokohama. pages 63–88, 1995.

[21] T.T. Soong and A.M. Reinhorn. Department of homeland security federal emergency management agency. page 701713, 1993.

[22] T.T. Soong and G.K. Skinner. Experimental study of active structural control. *Journal of Engineering Mechanics Division*, (Vol:113):1057–1067, July 1981.

[23] T.T.Soong and G.F Dargush. Passive energy dissipation systems in structural engineering. *University of New York at Buffalo, USA. John Willey & Sons*, 1997.